

NASA TECHNICAL NOTE



NASA TN D-4222

c. 1

NASA TN D-4222



TECH LIBRARY KAFB, NM

LOAN COPY: RETUR  
AFWL (WLIL-2)  
KIRTLAND AFB, N MEX

CORE EXCITATION IN SILVER,  
INDIUM, AND ANTIMONY RESULTING  
FROM INELASTIC SCATTERING OF  
42-MeV (6.7-pJ) ALPHA PARTICLES

*by William M. Stewart, Norton Baron, and Regis F. Leonard*

*Lewis Research Center  
Cleveland, Ohio*



0130891

NASA TN D-4222

CORE EXCITATION IN SILVER, INDIUM, AND ANTIMONY  
RESULTING FROM INELASTIC SCATTERING OF  
42-MeV (6.7-pJ) ALPHA PARTICLES

By William M. Stewart, Norton Baron, and Regis F. Leonard

Lewis Research Center  
Cleveland, Ohio

NATIONAL AERONAUTICS AND SPACE ADMINISTRATION

---

For sale by the Clearinghouse for Federal Scientific and Technical Information  
Springfield, Virginia 22151 - CFSTI price \$3.00

# CORE EXCITATION IN SILVER, INDIUM, AND ANTIMONY RESULTING FROM INELASTIC SCATTERING OF 42-MeV (6.7-pJ) ALPHA PARTICLES

by William M. Stewart, Norton Baron, and Regis F. Leonard

Lewis Research Center

## SUMMARY

Alpha particles of energy 42 MeV (6.7 pJ) have been elastically and inelastically scattered from isotopes of silver, indium, and antimony in an attempt to excite states which may be describable in terms of an excited core model. Angular distributions ( $30^\circ \leq \theta_{\text{cm}} \leq 80^\circ$ ) were measured for excited states of all nuclei. In each isotope, a number of states have been excited with cross sections of the right order of magnitude to indicate that they are collective in nature. The data obtained are compared with that for the appropriate neighboring even-even cores (palladium, cadmium, tin, or tellurium) with respect to the strength of the excitation, the excitation energy, and the multiplicity of states observed. It appears that fairly good agreement with the excited core model is obtained for indium and somewhat less good agreement for the isotopes of silver and antimony. The energy resolution of the present experiment prohibits any strong statements concerning the multiplicity of excited states.

## INTRODUCTION

In reference 1, de-Shalit proposed that, in odd  $A$  nuclei, there may exist excited states which may be described as arising from the coupling of the odd particle to a collective excitation of the even-even core. He described the low-lying excited states of silver, thallium, and gold as being of this type. The model has, since its proposal, been applied with varying degrees of success to copper 63, lead 207, and yttrium 89 (ref. 1). Most commonly, the states observed correspond to the coupling of an odd nucleon (or hole) to the one phonon  $2^+$  first excited state of the core. In lead 207, the two states have been seen (ref. 2) which appear to arise from the coupling of a  $3p_{1/2}$  neutron hole to a single phonon  $3^-$  state of lead 208.

In its simplest form, the weak coupling or core excitation model predicts that

(1) In the odd nucleus, there will be a multiplet of excited states which are collective in nature. The number of members of the multiplet will be  $2J_c + 1$  or  $2J_i + 1$  whichever is smaller. ( $J_c$  is the spin of the collective excitation in the even core and  $J_i$  is the ground state spin of the odd nucleus.) The spins of these states will be  $J_f$  where  $|J_c - J_i| \leq J_f \leq |J_c + J_i|$ .

(2) The center of gravity of the excitation energy of the multiplet should be approximately equal to the excitation energy of the collective state in the core.

(3) The electromagnetic transition probability to the ground state should be approximately equal to that for the collective state of the core. This implies that the cross section for inelastic scattering to any member of the multiplet should be proportional to  $2J_f + 1$  and that the total cross section for excitation of the multiplet should be equal to that for excitation of the collective state in the core. In addition, the angular distribution for each member of the multiplet should resemble that for excitation of the collective state of the core, that is, characterized by angular momentum transfer  $J_c$ .

In the present experiment, 42-MeV (6.7-pJ) alpha particles were scattered from silver 107 and 109, indium 113 and 115, and antimony 121 and 123 in an attempt to excite such collective core states, in particular, states corresponding to quadrupole, octupole, and two phonon core vibrations. Alpha particles seemed an ideal tool for this purpose since it is known that their inelastic scattering preferentially excites collective states. In addition, inelastic alpha scattering experiments have been performed on even tin (ref. 3) and tellurium (ref. 4) isotopes whose nuclei form the even-even cores for some of those presently under investigation. Such scattering data is useful for the analysis of the core excitations reported herein.

## SYMBOL LIST

a	diffuseness parameter in Woods-Saxon potential
$E^*$	excitation energy of nuclear level with respect to ground state of nucleus
$2d_{5/2}$	classification of nuclear state according to nuclear shell model
fwhm	full width at half maximum
$1g_{9/2}$	classification of nuclear state according to nuclear shell model
$1g_{7/2}$	classification of nuclear state according to nuclear shell model
$J_c$	spin of collective excitation of even core
$J_f$	excited state spin of odd nucleus
$J_i$	ground state spin of odd nucleus

$3p_{1/2}$	classification of nuclear state according to nuclear shell model
Q	excess of final kinetic energy over initial kinetic energy in nuclear reactions
$R_0$	nuclear radius constant
V	strength of real part of nuclear optical potential
W	strength of imaginary part of nuclear optical potential
$\beta_2$	deformation parameter for quadrupole vibrational state
$\beta_3$	deformation parameter for octupole vibrational state
$\beta_2^{J_f}$	partial deformation parameter for state of spin $J_f$ resulting from quadrupole vibrational excitation
$\theta_{cm}$	scattering angle of reaction product particle in center of mass system
$\theta_{lab}$	scattering angle of reaction product particle in laboratory system
$\pi$	parity of nuclear state
$\sigma_R$	total reaction cross section
$\left(\frac{d\sigma}{d\Omega}\right)_{J_f}^{exp}$	experimental differential cross section for spin state $J_f$
$\left(\frac{d\sigma}{d\Omega}\right)_{DRC}$	differential cross section calculated by direct reaction calculation
$\chi^2$	measure of statistical goodness of fit

## EXPERIMENTAL ARRANGEMENT

The external 42-MeV (6.7-pJ) alpha particle beam of the NASA, Lewis cyclotron was used in conjunction with a 64-inch (1.63-m) diameter scattering chamber for the present experiment. A schematic diagram of the scattering system is shown in figure 1. Details of the experimental arrangement are given elsewhere (refs. 3 and 4). As described in reference 4, a four detector mount was used which permitted the simultaneous measurement of cross sections at four different angles. The angular separation between detectors was  $4^\circ$ , and the angular resolution was approximately  $0.75^\circ$ . The detectors were lithium-drifted silicon produced at Lewis (ref. 5). The electronics were exactly as employed in reference 4. A block diagram is shown in figure 2. The overall energy resolution of the experiment was approximately 80 to 100 keV (13 to 16 fJ) for angles forward

of about  $55^\circ$  for all targets except  $^{109}\text{Ag}$ , whose thickness limited resolution. At back angles, the resolution was 100 to 120 keV (16 to 19 fJ). The incident beam energy was determined to be  $42.2 \pm 0.20$  MeV ( $6.76 \pm 0.03$  pJ) by the methods previously described (ref. 3). For all of the isotopes studied here, differential cross sections were measured for scattering angles between approximately  $30^\circ$  and  $80^\circ$ . This angular range was sufficient to establish the angular momentum transfer involved in the transition.

## ABSOLUTE CROSS SECTIONS

Absolute thickness measurements were made for the silver 107 and 109 ( $^{107}\text{Ag}$  and  $^{109}\text{Ag}$ ) and indium 115 ( $^{115}\text{In}$ ) targets by means of a transmission experiment with a naturally radioactive alpha emitting source, as outlined in reference 3. The thicknesses and isotopic abundances of these targets are listed in table I. Total error in the absolute cross sections for each of these three targets is estimated to be 10 percent. For the other three targets, indium 113 ( $^{113}\text{In}$ ) and antimony 121 and 123 ( $^{121}\text{Sb}$  and  $^{123}\text{Sb}$ ), such a determination of target thickness was impossible because of the presence of an impurity (mass number of approximately 30) in considerable abundance. Consequently, the cross sections quoted for these isotopes have been obtained by normalizing the relative values to some known cross section. For  $^{113}\text{In}$ , the elastic cross section was normalized to that for  $^{115}\text{In}$ , which was known absolutely. It is not expected that this will introduce an error of more than 10 percent, since, for a given element, the elastic cross sections of various isotopes have been observed to vary by less than this amount (refs. 3 and 4). For the antimony isotopes, absolute cross sections were obtained by normalizing the elastic scattering to the average elastic cross section of four tin and five tellurium isotopes. The maximum deviation of individual tin and tellurium isotopes from this average is less than 10 percent so that the error introduced into the antimony cross sections by this normalizing should be less than 20 percent. Consequently, the total error in the absolute cross sections for  $^{113}\text{In}$  and the antimony isotopes is estimated to be 15 and 25 percent, respectively. The cross sections obtained for all the isotopes, whether directly or indirectly (by normalizing to other data), are tabulated in tables II to VII. The errors quoted there are only the statistical uncertainty. In cases where cross sections are quoted for individual members of a closely spaced multiplet, there is an uncertainty as to exactly how the multiplet should be analyzed. This results in an additional error which is probably at least as large as the statistical error.

## EXCITATION ENERGIES

As in previous reports, excitation energies were obtained using the scattering from

the ground state and the well known first excited state ( $Q = -4.433$  MeV (710 fJ)) of carbon 12 as a calibration. Because four of the targets ( $^{113}\text{In}$ ,  $^{115}\text{In}$ ,  $^{121}\text{Sb}$ , and  $^{123}\text{Sb}$ ) were backed on 25 micrograms per centimeter squared of carbon, this calibration and the experimental run could be done simultaneously. For the silver targets, a thin film of oil gradually accumulated on the target which permitted the same procedure to be followed. In general, the excitation energies determined in this manner are accurate to  $\pm 15$  keV (2.4 fJ) for strongly excited single peaks. For very weak excitations, the method is limited by the inability to locate the peak accurately, and the error in the excitation energy may be as large as 50 keV (8.0 fJ).

## EXPERIMENTAL RESULTS

### Silver Isotopes

The silver isotopes should be the simplest to interpret. Silver may be considered to be either a palladium core plus a proton or as a cadmium core plus a proton hole. In either case, since the ground state spin of the silver nuclei is  $1/2$ , one expects a series of doublets corresponding to the weak coupling of this ground state spin to the collective excitations of the core. In particular, one expects a doublet of spins  $(3/2)^-$  and  $(5/2)^-$  near 500 keV (80 fJ) resulting from the one quadrupole phonon excitation of the core. These states are known in both silver isotopes and were among those used as examples by de-Shalit (ref. 1). The present work was intended to corroborate this knowledge and to look for other excitations of a similar type: in particular, those arising from the coupling of the odd proton (hole) to two-phonon excitations and octupole vibrations of the core. States of this type have been reported by Robinson, Ford, and Stelson in the inelastic scattering of 13-MeV (2.1-pJ) protons from  $^{107}\text{Ag}$  (ref. 6). Typical energy spectra from the present experiment are shown in figure 3 for  $^{107}\text{Ag}$  and  $^{109}\text{Ag}$ . The angular distributions for all states which could be analyzed are shown in figure 4. It was impossible to analyze those states in  $^{109}\text{Ag}$ , which correspond to the 780 keV (125 fJ) and 1140 keV (183 fJ) levels of  $^{107}\text{Ag}$ , because a thicker  $^{109}\text{Ag}$  target resulted in poorer energy resolution.

By far the strongest inelastic peak in both silver spectra is that near 400 keV (64 fJ). The angular distribution of this group is shown in figure 4 to be out of phase with the elastic angular distribution, as is typical for excitation of a quadrupole vibrational state. Inspection of figure 5 shows this peak to be a doublet, and, since the energies of the two states are known, it is possible to determine fairly accurately their relative strengths. The doublet was fit with the sum of two Gaussians, each of which has the same width as the elastic peak. The resultant decomposition is shown in figure 5 for both  $^{107}\text{Ag}$  and

<sup>109</sup>Ag. The dashed lines in figure 5 represent the individual members of the doublet; the solid line is the total. The experimental data are also shown. The strengths of the two levels involved were consistently in the ratio of 6 to 4, exactly as one would expect on the basis of a  $2J_f + 1$  proportionality. (The spins of these two states are 5/2 and 3/2.) There are unfortunately no data available on the scattering of alpha particles from palladium isotopes. There are available (ref. 7), however, values of the deformation parameter  $\beta_2$  for the first excited states of all the stable cadmium and palladium isotopes. For each state of the doublet in each isotope, a distorted wave Born approximation (DWBA) analysis (ref. 8) was done to extract a partial deformation parameter  $\beta_2^{J_f}$  defined by

$$\left(\frac{d\sigma}{d\Omega}\right)_{J_f}^{\text{exp}} = \left(\beta_2^{J_f}\right)^2 \left(\frac{d\sigma}{d\Omega}\right)_{\text{DWBA}} \quad (1)$$

where

$$\left(\frac{d\sigma}{d\Omega}\right)_{\text{DWBA}} = \frac{2J_i + 1}{2J_f + 1} \left(\frac{d\sigma}{d\Omega}\right)_{\text{DRC}} \quad (2)$$

Then, if the core excitation model is valid, it is true that (ref. 9)

$$\beta_2^{J_f} = \left[ \frac{2J_f + 1}{(2J_i + 1)(2J_c + 1)} \right]^{1/2} \beta_2(\text{core}) \quad (3)$$

and it follows that

$$[\beta_2(\text{core})]^2 = \sum_{J_f} \left(\beta_2^{J_f}\right)^2 \quad (4)$$

Determination of the optical model parameters used in the DWBA calculation is discussed in the appendix. The results of the DWBA calculation are shown with the data in figure 4. The partial deformation parameters  $\beta_2^{J_f}$  as well as the total deformation parameter  $\beta_2(\text{core})$  defined in equations (1) to (4) are listed in table VIII. Also listed are the deformation parameters measured by Stelson and McGowan (ref. 7) for cadmium

and palladium, and partial deformation parameters for both states of the silver 107 doublet (unpublished data by Ford, Wong, Tamura, Robinson, and Stelson of Oak Ridge National Laboratories). It is clear that excellent agreement exists. However, the errors in the total  $\beta_2$  obtained from the DWBA calculations are 10 to 15 percent and the errors in those of Stelson and McGowan are listed as 5 percent (ref. 7). Thus, it is not possible to say definitely whether the silver core resembles the palladium or the cadmium nucleus more strongly. The center of gravity energy of the doublet is  $380 \pm 15$  keV (61 fJ) for both  $^{107}\text{Ag}$  and  $^{109}\text{Ag}$ . These are also compared with the energies of the first excited states in the corresponding cadmium and palladium nuclei in table VIII. It is clear that the excitations are at a somewhat lower energy in both silver isotopes than the corresponding excitations in either palladium or cadmium. However, for both of the silver isotopes, they lie closer to the palladium than to the cadmium.

In both silver nuclei a number of somewhat weaker excitations were observed at energies between 0.500 and 2.0 MeV (80.1 and 320 fJ). The intensities of these peaks and the energy resolution of the experiment made it impossible to analyze all these states. In  $^{107}\text{Ag}$ , differential cross sections were obtained for states at excitation energies of 0.780, 0.953, and 1.14 MeV (125, 152, and 183 fJ). These are shown with the other  $^{107}\text{Ag}$  data in figure 4(a). The angular distributions for all three of these states are similar, and they appear to exhibit a slight shift such that they are neither exactly in nor out of phase with the elastic scattering. Unpublished results of 42-MeV (6.7-pJ) alpha scattering from even cadmium isotopes indicate a similar shift of the angular distribution for scattering to two phonon states. The magnitudes of these  $^{107}\text{Ag}$  cross sections are smaller by a factor of about 5 than for either member of the single-phonon doublet. This relative magnitude is typical of a two-phonon excitation. All this indicates that these states arise from the coupling of the odd particle (or hole) to a two-phonon excitation of the core. This is consistent with the findings of Robinson, Ford, and Stelson (ref. 6), who report that the cross sections for inelastic proton scattering to the 0.953- and 1.14-MeV (152 and 183 fJ) levels are similar to those for scattering to the two-phonon state of  $^{106}\text{Pd}$ . Only one state in this energy range at 0.860 MeV (138 fJ) could be analyzed for  $^{109}\text{Ag}$ , because of the poorer energy resolution and slightly closer level spacing. The differential cross section for this one state was similar to that for the 0.953 MeV (152 fJ) state in  $^{107}\text{Ag}$  both in shape and magnitude, so that, presumably, it is a similar type of excitation.

In addition, states were seen in both silver nuclei at an energy of 2.17 MeV (348 fJ), which possessed an angular distribution characteristic of an angular momentum transfer of 3. These states can be associated with the coupling of the odd proton (or hole) to an octupole vibration of the core. This observed excitation energy is fairly close to reported excitation energies for spin three states in both palladium (ref. 9) and cadmium (ref. 10). These energies are listed in table IX. In neither of the octupole states in

silver can any positive indication be seen of a splitting, such as one would expect on the basis of the weak coupling model. If the states in question are doublets, then the separation between the members of the doublet must be less than 60 keV (9.6 fJ), otherwise it would manifest itself at least as a broadening of the peak in the present experiment. The partial deformation parameters obtained for these states are listed in table IX. These values are approximately what is expected for one member of the  $3^-$  doublet. For example,  $\beta_3^{J_f} = 0.10$  for  $^{107}\text{Ag}$ . The value of  $\beta_3$  for  $^{106}\text{Pd}$  is reported (ref. 9) to be 0.15 and that for  $^{108}\text{Cd}$  should be approximately the same (ref. 10). Therefore, on the basis of the weak coupling model, partial values of  $\beta_3^{5/2} = 0.10$  and  $\beta_3^{7/2} = 0.11$  are expected. Nowhere in the silver spectra, however, were there states with sufficient strength to account for the remaining octupole strength. A summary of all the states excited in both silver isotopes is shown in figure 6.

## Indium Isotopes

Indium is considerably more complicated than silver since the ground state spins of both stable indium nuclei are  $9/2^+$ . The last proton of the indium nuclei is situated in the  $1g_{9/2}$  shell. Consequently, indium may be considered as either a tin core plus a proton hole or a cadmium core plus a proton. Because of the large spin of the ground state, the one quadrupole-phonon core excitation is expected to split into five components with spins  $5/2$ ,  $7/2$ ,  $9/2$ ,  $11/2$ , and  $13/2$ . The octupole vibrational state will be split into seven components with spins  $3/2$ ,  $5/2$ ,  $7/2$ ,  $9/2$ ,  $11/2$ ,  $13/2$ , and  $15/2$ . It was expected that the energy resolution possible in the present experiment would not be capable of completely resolving these multiplets. Typical energy spectra for  $^{113}\text{In}$  and  $^{115}\text{In}$  are shown in figure 7. Two rather strong groups are immediately obvious, one near 1.2 MeV (192 fJ) and one near 2.4 MeV (384 fJ). These two multiplets were analyzed to determine whether they could be interpreted as vibrational core excitations.

It was first determined that all the states excited near 1.2 MeV (192 fJ) were similar in nature and that all those near 2.4 MeV (384 fJ) were similar. This is shown in figure 8, where the angular distributions for the five most prominent components of the  $^{113}\text{In}$  spectrum (1.17, 1.36, 1.56, 2.17, and 2.48 MeV or 187, 218, 250, 348, and 397 fJ) are shown. It is clear that the 1.17-, 1.36-, and 1.56-MeV (187-, 218-, and 250-fJ) peaks are out-of-phase with the elastic angular distribution, and that the relative strengths of the three are approximately independent of angle. Consequently, the entire group will be treated together. Similarly, the 2.17- and 2.48-MeV (348- and 397-fJ) states are in phase with the elastic cross section and will be treated as a unit. The angular distributions of the corresponding groups of  $^{115}\text{In}$  exhibit the same behavior.

The sum of the strengths of the 1.17-, 1.36-, and 1.56-MeV (187-, 218-, and 250-fJ) peaks in the  $^{113}\text{In}$  spectrum is plotted in figure 9(a), and compared with that for the first

excited (the one quadrupole-phonon) state of the tin core. (The tin cross sections shown here are for  $^{116}\text{Sn}$ . The most appropriate for comparison with  $^{113}\text{In}$  would be  $^{114}\text{Sn}$ . These data are not available; however, it is known that neither quadrupole nor octupole cross sections vary very rapidly with neutron number for the tin isotopes, see ref. 3.) It is clear that the total strength is, within experimental error, equal to the tin cross section, as required by the weak coupling model. Also shown in figure 9(a) is the total strength of the multiplet near 2.4 MeV (385 fJ). It is compared with the cross section for excitation of the one octupole-phonon ( $3^-$ ) state in  $^{116}\text{Sn}$ . Again it is clear that, within experimental error, the tin and indium cross sections are equal. A similar comparison of  $^{115}\text{In}$  and  $^{116}\text{Sn}$  is shown in figure 9(b). The same conclusions may be drawn.

It is also interesting to determine whether the number of peaks in each multiplet is that expected on the basis of the core excitation model. It is clear that the resolution obtained in the present experiment does not permit an absolute answer to this question; however, some limits may be set by close examination of the energy spectra. From figure 7(a), the  $^{113}\text{In}$  group at 1.17 MeV (187 fJ) is at least a doublet. In fact, there have been four states reported at excitation energies of 1.120, 1.176, 1.374, and 1.590 MeV (179.3, 188.2, 220.1, and 254.5 fJ) (ref. 11). On the basis of the data presented herein, one could not eliminate the possible existence of a fifth member of the  $2^+$  multiplet. However, the study of reference 11 had a resolution of several keV and did not indicate the existence of any other state except for one at 1.026 MeV (164.2 fJ). This state was definitely not excited in this investigation, and hence, is probably not the result of a core excitation. High resolution studies of the  $3^-$  multiplet have not been reported; therefore, it is more difficult to identify individual peaks.

For  $^{115}\text{In}$ , a more detailed analysis has been made for both the  $2^+$  and the  $3^-$  multiplets based on the following assumptions:

(1) The individual lines of the multiplet have Gaussian shapes with a width equal to that displayed by the elastically scattered alpha particles.

(2) The individual components have intensities proportional to  $2J_f + 1$ , as required by the weak-coupling model.

(3) Previous reports of excitation energies are correct (refs. 11 to 14). In particular, it was assumed that states existed at energies of 1.080 ( $5/2^+$ ), 1.125 ( $13/2^+$ ), 1.285 ( $11/2^+$ ), and 1.420 ( $9/2^+$ ) MeV (173.1, 180.2, 206.0, and 227.6 fJ). A previously reported state at 0.935 MeV (149.7 fJ) was not included because it was not excited with any significant cross section.

Such analysis is shown in figure 10(a) where the dashed lines are members of the multiplet and the solid line is the total, which includes a flat background of 50 counts. It is possible to add another state of 1.10 MeV (176 fJ) with a spin of  $7/2$  and improve the fit to the experimental spectrum as shown in figure 10(b). Hence, it is clear that all five members of the multiplet may be present. However, it is true that gamma ray spectra

with much higher energy resolution (ref. 13) than the present experiment have failed to indicate the presence of the fifth level ( $7/2^+$ ), so that the evidence presented here should be considered as rather weak.

A similar construction is shown in figure 11 for the  $3^-$  multiplet of  $^{115}\text{In}$  with states at 1.94 ( $5/2^-$ ), 2.05 ( $9/2^-$ ), 2.11 ( $13/2^-$ ), 2.29 ( $7/2^-$ ), 2.34 ( $3/2^-$ ), 2.41 ( $11/2^-$ ), and 2.46 ( $15/2^-$ ) MeV (311, 328, 338, 367, 375, 386, and 394 fJ). Again, it indicates only the possible existence of a multiplet of seven states, and should not be taken to indicate the existence or excitation energy of any one particular state.

Also, the center of gravity of each multiplet was computed. The energy calibration was done in the same manner as for the silver (the indium targets were mounted on carbon backings). The results of these calculations are shown in table X. There is excellent agreement with the energy levels of the tin isotope, poorer agreement with those of the cadmium isotope. A summary of all the indium levels is shown in figure 12.

## ANTIMONY ISOTOPES

Antimony is the most complicated of the isotopes reported herein. The ground state spin of  $^{121}\text{Sb}$  is  $(5/2)^+$  so that the core quadrupole excitation will be split into five components and the octupole into six. For  $^{123}\text{Sb}$  the ground state spin is  $(7/2)^+$  so that the quadrupole excitation results in five states, the octupole in seven. Typical energy spectra for  $^{121}\text{Sb}$  and  $^{123}\text{Sb}$  are shown in figure 13. In  $^{121}\text{Sb}$ , groups were observed at 0.545, 1.04, and 1.15 MeV (87.4, 166.8, and 184.1 fJ). In  $^{123}\text{Sb}$  a similar spectrum was observed with states at 0.549 MeV (87.9 fJ) and an unresolved doublet at 1.08 MeV (173.2 fJ). All these groups displayed a differential cross section typical of a quadrupole excitation (fig. 14). States of  $^{121}\text{Sb}$  were reported previously by Barnes, et al. (ref. 15) at 0.506, 0.573, 1.024, and 1.143 MeV (81.2, 91.7, 164.2, and 183.2 fJ). They also reported states in  $^{123}\text{Sb}$  at 0.541, 1.029, 1.087, and 1.181 MeV (86.7, 164.8, 174.1, and 189.2 fJ). Of these, the states near 0.550 MeV (88.1 fJ) in both isotopes are not perfect weak-coupling excitations since Barnes, et al. reported rather large spectroscopic factors as measured in ( $^3\text{He}, d$ ) reactions. However, the cross sections for inelastic alpha scattering indicate that, in this respect, they are weak-coupling states. The total quadrupole strength of each antimony isotope is compared in figure 15 with the strengths of the first  $2^+$  states in the corresponding tin and tellurium isotopes. The antimony  $2^+$  multiplet agrees better with the tin cross sections than with the tellurium.

Two other groups were excited in  $^{121}\text{Sb}$ . The first of these was centered about an energy of 2.26 MeV (362 fJ). The width of this group (0.450 MeV; 72.3 fJ) would require the presence of at least five states. The angular distribution of this group (fig. 14) is in phase with that of the elastic scattering, indicating that these states may be mem-

bers of an octupole excitation. In figure 15, this cross section is compared with those of the octupole states in  $^{120}\text{Sn}$  and  $^{122}\text{Te}$  and is found to agree well with both. The  $3^-$  group of  $^{123}\text{Sb}$  was not observed because of the presence of an impurity.

The other state in  $^{121}\text{Sb}$  was observed at an excitation energy of 1.42 MeV (227 fJ). Its angular distribution (fig. 14) could not be classified as either in or out of phase with the elastic scattering. Consequently, it is not included in the total strengths of either the  $2^+$  or the  $3^-$  multiplets shown in figure 15.

The centers of gravity of the two multiplets are listed in table XI. The quadrupole multiplets are closer to the  $2^+$  level of tin. However, the octupole groups of  $^{121}\text{Sb}$  agree equally well with either tin or tellurium. A summary of all the antimony levels is shown in figure 16.

## DISCUSSION

All the isotopes studied here exhibit states classifiable as core excitations. In the silver nuclei, two states were seen which have the proper angular distribution, strength, and excitation energy to be the result of the coupling of a proton (or hole) to the one quadrupole phonon excitation of the core. Also a state was seen at the proper excitation energy with the right differential cross section to be classified as one member of a doublet resulting from an octupole excitation of the core. However, the remainder of the octupole strength was not seen in either silver isotope. In addition, a number of weakly excited states were seen whose energies and angular distributions indicate that they may result from excitation of two phonon states of the even core. Nothing observed in the present experiment indicates whether the silver cores resemble more strongly a palladium or a cadmium nucleus. The information is summarized in tables VIII and IX, and figures 4 and 6.

The indium isotopes can be described quite well in terms of a core excitation model. Two multiplets were seen whose total strengths, angular distributions, and centers of gravity are in excellent agreement with the corresponding quantities in the even tin neighbor. The only respect in which the weak coupling model might appear to be deficient in its description of the indium nuclei is in the number of members of the multiplet. The work reported herein, however, cannot make any definite statement in this regard. It does seem clear on the basis of the present work that the cores of the odd indium isotopes resemble the tin isotopes much more strongly than they do the cadmium. This is most noticeable in the comparison of the excitation energies. This information is summarized in table X and figures 9 and 12.

The antimony isotopes clearly bear some resemblance to a core excited nucleus. A number of states (probably 3 or 4) are seen which have the angular distribution and almost the strength expected for a core quadrupole excitation. A group of states is seen

which resembles an octupole multiplet. The quadrupole multiplet, however, is split with an appreciable part of it appearing at a lower energy (0.550 MeV; 88.1 fJ). This information is summarized in table XI and figures 15 and 16. In addition, these states have a rather large amount of single-particle character as indicated by the ( $^3\text{He}, d$ ) studies (ref. 15). Very likely these deviations from the model are due to the existence of a very low-lying single-particle state in each of the antimony isotopes. This is the  $1g_{7/2}$  state (0.035 MeV; 5.61 fJ) in  $^{121}\text{Sb}$  and the  $2d_{5/2}$  state (0.160 MeV; 25.6 fJ) in  $^{123}\text{Sb}$ . The existence of such a low-lying single particle level could destroy the weak coupling between the odd particle (hole) and core thus causing considerable deviations from the predictions of the simple model. Several authors (refs. 16 to 18) have treated this problem and have attempted to calculate the expected energy levels including the effects of possible admixtures of other low-lying single particle states. A higher resolution study of these isotopes would be necessary to study individual members of the multiplets excited herein.

Lewis Research Center,  
National Aeronautics and Space Administration,  
Cleveland, Ohio, May 11, 1967,  
129-02-04-06-22.

## APPENDIX - OPTICAL MODEL PARAMETERS

The optical model parameters used in the DWBA calculation (ref. 8) were obtained from the analysis of the elastic scattering using the optical model program of Melkanoff, et al. (ref. 19). The nuclear part of the optical potential was assumed to have a Woods-Saxon radial form factor using the same radius and diffuseness for both the real and imaginary part of the potential

$$U(r) = -(V + iW) \left[ 1 + \exp\left(\frac{r - R_0 A^{1/3}}{a}\right) \right]^{-1}$$

It is known from previously reported works (refs. 3 and 4) that a continuous set of equivalently good optical model parameters could be found for scattering of 42-MeV (6.7-pJ) alpha particles from tin and tellurium isotopes. Thus, for these calculations, the value of the nuclear radius parameter  $R_0$  was fixed at 1.45 fm and the computer program optimized the three parameters  $V$ ,  $W$ , and  $a$  by minimizing the quantity  $\chi^2$ . A tabulation of these parameters resulting from these searches is given as follows:

Target	Strength of real part of nuclear optical potential, $V$		Strength of imaginary part of nuclear optical potential, $W$		Diffuseness parameter in Woods-Saxon potential, $a$ , fm	Nuclear radius constant, $R_0$ , fm	Total reaction cross section, $\sigma_{R'}$ , fm <sup>2</sup>	Goodness of fit per data point, $\chi^2/N$
	MeV	pJ	MeV	pJ				
<sup>107</sup> Ag	59.99	9.61	25.04	4.01	0.6605	1.45	181.5	1.82
<sup>109</sup> Ag	55.57	8.90	28.31	4.54	.7047	↓	190.2	1.69
<sup>113</sup> In	53.35	8.55	26.70	4.28	.6645		182.9	2.45
<sup>115</sup> In	54.67	8.76	27.41	4.39	.6744		188.2	1.23
<sup>121</sup> Sb	56.23	9.01	28.88	4.61	.6594		190.0	.425
<sup>123</sup> Sb	54.56	8.74	27.09	4.33	.6442		186.8	.975

## REFERENCES

1. de-Shalit, A.: Core Excitations in Nondeformed, Odd-A, Nuclei. *Phys. Rev.*, vol. 122, no. 5, June 1, 1961, pp. 1530-1536.
2. Hafele, Joseph C.; and Blair, A. G.: Observation of the Doublet Splitting of the 2.6-MeV Octupole State of  $\text{Pb}^{207}$ . *Am. Phys. Soc. Bull.*, ser. II, vol. 11, no. 1, Jan. 1966, p. 12.
3. Baron, Norton; Leonard, Regis F.; Need, John L.; and Stewart, William M.: Elastic and Inelastic Scattering of 40-MeV Alpha Particles from Even Tin Isotopes. NASA TN D-3067, 1965.
4. Leonard, Regis F.; Stewart, William M.; and Baron, Norton: Elastic and Inelastic Scattering of 42-MeV Alpha Particles from Even Tellurium Isotopes. NASA TN D-3991, 1967.
5. Baron, Norton; and Kaminski, Gerald A.: Manufacture of Lithium-Drifted Silicon Surface-Barrier Semiconductor Counters. NASA TN D-3554, 1966.
6. Robinson, R. L.; Ford, J. L. C.; and Stelson, P. H.: Inelastic Scattering of Protons from  $^{106}\text{Pd}$ ,  $^{107}\text{Ag}$ ,  $^{108}\text{Pd}$ , and  $^{112}\text{Cd}$ . *Am. Phys. Soc. Bull.*, ser. II, vol. 11, no. 1, Jan. 1966, p. 119.
7. Stelson, P. H.; and McGowan, F. K.: Coulomb Excitation of Medium-Weight Even-Even Nuclei. *Phys. Rev.*, vol. 110, no. 2, Apr. 15, 1958, pp. 489-506.
8. Gibbs, W. R.; Madsen, V. A.; Miller, J. A.; Tobocman, W.; Cox, E. C.; and Mowry, L.: Direct Reaction Calculation. NASA TN D-2170, 1964.
9. Robinson, R. L.; Ford, J. L. C., Jr.; Stelson, P. H.; and Satchler, G. R.: Elastic and Inelastic Proton Scattering from  $^{106}\text{Pd}$  and  $^{108}\text{Pd}$ . *Phys. Rev.*, vol. 146, no. 3, June 17, 1966, pp. 816-823.
10. McGowan, F. K.; Robinson, R. L.; Stelson, P. H.; Ford, J. L. C.; and Milner, W. T.: Coulomb Excitation of Vibrational Triplet States and Octupole States in the Even Cadmium Nuclei. *Am. Phys. Soc. Bull.*, ser. II, vol. 9, no. 1, Jan. 1964, p. 107.
11. Bernstein, E. M.; Seaman, G. G.; and Palms, J. M.: Coulomb Excitation of  $^{113}\text{In}$  and  $^{115}\text{In}$  with Oxygen Ions. *Am. Phys. Soc. Bull.*, ser. II, vol. 12, no. 1, Jan. 1967, p. 19.
12. Pandharipande, V. R.; Sharma, R. P.; and Chandra, Girish: Angular Correlation Measurements in the Decay of  $\text{Cd}^{115\text{m}}$ . *Phys. Rev.*, vol. 136, no. 2B, Oct. 26, 1964, pp. 346-350.

13. Graeffe, G.; Tang, C. -W.; Coryell, C. D.; and Gordon, G. E.: Decay Schemes of 43-Day  $^{115m}\text{Cd}$  and 2.3-Day  $^{115g}\text{Cd}$ . Phys. Rev., vol. 149, no. 3, Sept. 23, 1966, pp. 884-893.
14. Sharp, R. D.; and Buechner, W. W.: Angular Distributions of Elastically and Inelastically Scattered Protons from Indium. Phys. Rev., vol. 112, no. 3, Nov. 1, 1958, pp. 897-902.
15. Barnes, P. D.; Ellegaard, C.; Herskind, B.; and Joshi, M. C.: Properties of Levels in  $^{121}\text{Sb}$  and  $^{123}\text{Sb}$  Excited with the Reactions ( $^3\text{He}, d$ ), ( $d, d'$ ), and ( $^{16}\text{O}, ^{16}\text{O}'\gamma$ ). Phys. Letters, vol. 23, no. 4, Oct. 24, 1966, pp. 266-269.
16. Thankappan, V. K.; and True, William W.: Properties of Low-Lying  $\text{Cu}^{63}$  Levels. Phys. Rev., vol. 137, no. 4B, Feb. 23, 1965, pp. 793-799.
17. Thankappan, V. K.:  $\text{Al}^{27}$  and the Excited-Core Model. Phys. Rev., vol. 141, no. 3, Jan. 1966, pp. 957-961.
18. Dang, Gin Do: Collective Excitations in Spherical Odd-Mass Nuclei. Nucl. Phys., vol. 62, 1965, pp. 153-164.
19. Melkanoff, Michel A.; Nodvik, John S.; Saxon, David S.; and Cantor, David G.: A FORTRAN Program for Elastic Scattering Analyses with the Nuclear Optical Model. University of California Press, 1961.

TABLE I. - DESCRIPTION OF TARGETS

Isotope	Enrichment, percent	Thickness		Thickness, mg/cm <sup>2</sup>
		keV	fJ	
Silver 107	98.9	128.3	20.55	0.546
Silver 109	99.1	515.7	82.62	2.197
Indium 115	99.99	108.3	173.5	.477

TABLE II. - DIFFERENTIAL CROSS SECTIONS FOR SCATTERING OF 42-MeV ALPHA PARTICLES BY SILVER 107

(a) Elastic scattering

Center-of-mass scattering angle, $\theta_{cm}$ , deg	Differential cross section, $d\sigma/d\Omega$ , fm <sup>2</sup> /sr	Center-of-mass scattering angle, $\theta_{cm}$ , deg	Differential cross section, $d\sigma/d\Omega$ , fm <sup>2</sup> /sr	Center-of-mass scattering angle, $\theta_{cm}$ , deg	Differential cross section, $d\sigma/d\Omega$ , fm <sup>2</sup> /sr
31.32	20.2 ± 0.0	47.79	0.466 ± 0.009	64.14	0.0684 ± 0.0011
33.38	16.1 ± .0	49.84	.593 ± .003	66.17	.0155 ± .0005
35.45	8.20 ± .02	51.89	.582 ± .010	68.20	.00906 ± .00040
37.51	4.00 ± .02	53.94	.333 ± .003	70.23	.0258 ± .0007
39.57	3.07 ± .01	55.98	.109 ± .005	72.26	.0321 ± .0008
41.63	3.06 ± .01	58.02	.0710 ± .0012	74.28	.0197 ± .0006
43.68	2.01 ± .01	60.06	.128 ± .005	76.30	.00613 ± .00033
45.74	.927 ± .007	62.10	.136 ± .002	78.32	.00087 ± .00013

(b) Inelastic scattering to 0.380-MeV (60.9-fJ) 2<sup>+</sup> doublet

31.32	0.333 ± 0.004	49.85	0.0515 ± 0.0010	66.18	0.0387 ± 0.0008
33.39	.137 ± .003	51.90	.0122 ± .0016	68.21	.0318 ± .0008
35.45	.499 ± .005	53.94	.0513 ± .0010	70.24	.00689 ± .00036
39.57	.329 ± .004	55.90	.112 ± .005	72.27	.00092 ± .00013
41.63	.0530 ± .0018	58.03	.0640 ± .0011	74.29	.00593 ± .00033
43.69	.124 ± .002	60.07	.0211 ± .0020	76.31	.0130 ± .0005
45.74	.268 ± .004	62.11	.00350 ± .0003	78.33	.0123 ± .0005
47.80	.236 ± .007	64.15	.0221 ± .0006		

(c) Inelastic scattering to 0.780-MeV (125-fJ) level

31.08	0.0514 ± 0.0015	49.61	0.00391 ± 0.00028	63.91	0.00041 ± 0.00009
33.15	.0414 ± .0016	51.66	.00312 ± .00058	65.95	.00043 ± .00009
37.27	.0146 ± .0009	53.71	.00217 ± .00021	67.98	.00050 ± .00010
39.33	.0184 ± .0009	55.75	.00066 ± .00025	70.01	.00059 ± .00010
41.39	.0121 ± .0009	57.80	.00162 ± .00018	74.06	.00025 ± .00007
45.51	.00245 ± .00039	59.84	.00125 ± .00039	76.08	.00004 ± .00003
47.56	.00319 ± .00056	61.88	.00097 ± .00014	78.10	.00011 ± .00004

TABLE II. - Concluded. DIFFERENTIAL CROSS SECTIONS FOR SCATTERING OF  
42-MeV ALPHA PARTICLES BY SILVER 107

(d) Inelastic scattering to 0.953-MeV (152-fJ) level

Center-of-mass scattering angle, $\theta_{cm}$ , deg	Differential cross section, $d\sigma/d\Omega$ , fm <sup>2</sup> /sr	Center-of-mass scattering angle, $\theta_{cm}$ , deg	Differential cross section, $d\sigma/d\Omega$ , fm <sup>2</sup> /sr	Center-of-mass scattering angle, $\theta_{cm}$ , deg	Differential cross section, $d\sigma/d\Omega$ , fm <sup>2</sup> /sr
31.33	0.0532 ± 0.0015	49.86	0.0195 ± 0.0006	66.20	0.00191 ± 0.00019
33.40	.0202 ± .0011	51.91	.0111 ± .0015	68.23	.00301 ± .00023
35.46	.0225 ± .0010	53.96	.0026 ± .0002	70.26	.00358 ± .00026
39.58	.0399 ± .0013	56.00	.0041 ± .0008	72.28	.00313 ± .00024
41.64	.0313 ± .0014	58.04	.0092 ± .0004	74.31	.00112 ± .00014
43.70	.0102 ± .0007	60.09	.0089 ± .0010	76.33	.00063 ± .00011
45.75	.0159 ± .0010	62.12	.00465 ± .00031	78.35	.00124 ± .00015
47.81	.0249 ± .0021	64.16	.00127 ± .00015		

(e) Inelastic scattering to 1.14-MeV (183-fJ) level

31.09	0.0675 ± 0.0171	49.62	0.00925 ± 0.00043	63.92	0.00109 ± 0.00014
33.15	.0349 ± .0015	51.67	.00685 ± .00087	65.96	.00102 ± .00014
37.28	.0275 ± .0013	53.72	.00242 ± .00021	67.99	.00142 ± .00016
39.34	.0282 ± .0011	55.76	.00175 ± .00044	70.02	.00254 ± .00021
41.40	.0244 ± .0012	57.80	.00370 ± .00027	74.04	.00098 ± .00013
45.51	.00673 ± .00064	59.85	.00428 ± .00068	76.09	.00035 ± .00008
47.57	.00959 ± .00108	61.88	.00350 ± .00026	78.11	.00046 ± .00009

(f) Inelastic scattering to 2.17-MeV (348-fJ) level

31.35	0.243 ± 0.003	49.88	0.0289 ± 0.0007	66.23	0.00378 ± 0.00026
33.42	.190 ± .003	51.93	.0338 ± .0020	68.26	.00453 ± .00029
35.48	.0555 ± .0016	53.98	.0201 ± .0006	70.29	.00491 ± .00030
39.60	.0554 ± .0016	56.03	.0116 ± .0012	72.32	.00355 ± .00025
41.66	.0828 ± .0023	58.07	.0058 ± .0003	74.34	.00332 ± .00025
43.72	.0506 ± .0015	60.11	.0122 ± .0012	76.36	.00202 ± .00019
45.78	.0227 ± .0012	62.15	.00856 ± .00041	78.38	.00074 ± .00012
47.83	.0221 ± .0017	64.19	.00780 ± .00038		

TABLE III. - DIFFERENTIAL CROSS SECTIONS FOR SCATTERING OF 42-MeV ALPHA

PARTICLES BY SILVER 109

(a) Elastic scattering

Center-of-mass scattering angle, $\theta_{cm}$ , deg	Differential cross section, $d\sigma/d\Omega$ , $fm^2/sr$	Center-of-mass scattering angle, $\theta_{cm}$ , deg	Differential cross section, $d\sigma/d\Omega$ , $fm^2/sr$	Center-of-mass scattering angle, $\theta_{cm}$ , deg	Differential cross section, $d\sigma/d\Omega$ , $fm^2/sr$
31.30	21.4 ± 0.0	47.76	0.507 ± 0.003	64.10	0.0562 ± 0.0006
33.36	16.0 ± .0	49.81	.597 ± .003	66.14	.0146 ± .0003
35.42	8.67 ± .02	51.86	.550 ± .003	68.17	.0116 ± .0003
37.48	4.07 ± .01	53.91	.291 ± .002	70.20	.0294 ± .0004
39.54	3.24 ± .01	55.95	.0966 ± .0013	72.22	.0270 ± .0004
41.60	3.05 ± .01	57.99	.0835 ± .0012	74.25	.0162 ± .0003
43.66	2.02 ± .01	60.03	.130 ± .002	76.27	.00401 ± .00016
45.71	.875 ± .004	62.07	.118 ± .001	78.29	.00151 ± .00010

(b) Inelastic scattering to 0.380-MeV (60.9-fJ)  $2^+$  doublet

31.30	0.378 ± 0.004	47.77	0.211 ± 0.002	64.11	0.0241 ± 0.0004
33.37	.101 ± .002	49.82	.0533 ± .0009	66.14	.0318 ± .0005
35.43	.498 ± .004	51.87	.00381 ± .00025	68.18	.0175 ± .0004
37.49	.581 ± .004	53.91	.0469 ± .0009	72.23	.00070 ± .00007
39.55	.302 ± .003	55.96	.0967 ± .0013	74.25	.00433 ± .00017
41.61	.0354 ± .0009	58.00	.0626 ± .0010	76.27	.0119 ± .0003
43.66	.108 ± .002	60.04	.0136 ± .0005	78.29	.0104 ± .0003
45.71	.250 ± .002	62.08	.00360 ± .00025		

(c) Inelastic scattering to 0.860-MeV (138-fJ) level

31.31	0.0567 ± 0.0014	45.73	0.00895 ± 0.00043	60.05	0.00501 ± 0.00029
33.38	.0149 ± .0006	47.78	.01454 ± .0005	62.09	.00167 ± .00017
35.44	.0126 ± .0007	49.83	.0104 ± .0004	64.12	.00082 ± .00007
37.50	.0278 ± .0008	51.88	.00119 ± .00014	66.16	.00093 ± .00008
39.56	.0337 ± .0011	53.92	.00195 ± .00018	72.24	.00019 ± .00004
41.62	.0148 ± .0006	55.97	.00391 ± .00025	74.27	.00057 ± .00006
43.67	.0064 ± .0005	58.01	.00387 ± .00025		

(d) Inelastic scattering to 2.17-MeV (348-fJ) level

31.33	0.129 ± 0.002	45.75	0.0109 ± 0.0005	60.08	0.00697 ± 0.00034
33.39	.107 ± .002	47.80	.0051 ± .0003	62.12	.00651 ± .00033
35.46	.0501 ± .0013	49.85	.0152 ± .0005	64.16	.00350 ± .00015
37.52	.0169 ± .0006	51.90	.0188 ± .0006	66.19	.00164 ± .00011
39.58	.0386 ± .0011	53.95	.0115 ± .0004	72.28	.00188 ± .00011
41.64	.0552 ± .0011	56.00	.00288 ± .00022	74.30	.00174 ± .00011
43.69	.0390 ± .0011	58.04	.00348 ± .00024		

TABLE IV. - DIFFERENTIAL CROSS SECTIONS FOR SCATTERING OF 42-MeV ALPHA  
PARTICLES BY INDIUM 113<sup>a</sup>

(a) Elastic scattering

Center-of-mass scattering angle, $\theta_{cm}$ , deg	Differential cross section, $d\sigma/d\Omega$ , fm <sup>2</sup> /sr	Center-of-mass scattering angle, $\theta_{cm}$ , deg	Differential cross section, $d\sigma/d\Omega$ , fm <sup>2</sup> /sr	Center-of-mass scattering angle, $\theta_{cm}$ , deg	Differential cross section, $d\sigma/d\Omega$ , fm <sup>2</sup> /sr
41.08	3.11 ± 0.01	57.46	0.0987 ± 0.0017	73.71	0.0255 ± 0.0010
43.13	2.57 ± .01	59.50	.124 ± .002	75.73	.0111 ± .0005
45.19	1.41 ± .01	61.54	.145 ± .002	77.75	.00319± .00040
47.24	.643 ± .005	63.57	.0867 ± .0016	79.77	.00597± .00040
49.28	.569 ± .006	65.60	.0334 ± .0010	81.78	.00828± .00058
51.33	.640 ± .005	67.63	.0174 ± .0007	83.79	.00788± .00046
53.38	.468 ± .005	69.66	.0308 ± .0010	85.80	.00402± .00040
55.42	.214 ± .0030	71.69	.0364 ± .0010	87.81	.00128± .00018

(b) Inelastic scattering to 1.17-MeV (187-fJ) level

28.74	0.477 ± 0.004	51.35	0.00866± 0.00060	65.63	0.00746± 0.00050
36.99	.158 ± .002	53.40	.00811± .00070	67.66	.00669± .00040
41.10	.0512 ± .0012	55.44	.0167 ± .0008	69.69	.00450± .00040
43.15	.0169 ± .0008	57.48	.0204 ± .0008	71.71	.00097± .00020
45.21	.0443 ± .0017	59.52	.0099 ± .0005	73.74	.00115± .00020
47.26	.0549 ± .0015	61.56	.0020 ± .0002	75.76	.00166± .00020
49.31	.0358 ± .0015	63.60	.00297± .00030		

(c) Inelastic scattering to 1.36-MeV (218-fJ) level

28.74	0.185 ± 0.002	51.36	0.00862± 0.00061	65.63	0.00277± 0.00029
36.99	.0712 ± .0014	53.40	.00461± .00054	67.66	.00542± .00040
41.10	.0272 ± .0011	55.45	.00948± .00064	69.69	.00278± .00029
43.16	.0130 ± .0008	57.49	.0128 ± .0006	71.72	.00061± .00014
45.21	.0199 ± .0011	59.53	.00618± .00043	73.74	.00070± .00017
47.26	.0266 ± .0011	61.57	.00207± .00025	75.76	.00109± .00017
49.31	.0206 ± .0011	63.60	.00180± .00023		

<sup>a</sup> Absolute cross sections obtained by normalizing <sup>113</sup>In elastic to <sup>115</sup>In elastic cross sections.

TABLE IV. - Concluded. DIFFERENTIAL CROSS SECTIONS FOR SCATTERING OF

42-MeV ALPHA PARTICLES BY INDIUM 113<sup>a</sup>

(d) Inelastic scattering to 1.56-MeV (250 fJ) level

Center-of-mass scattering angle, $\theta_{cm}$ , deg	Differential cross section, $d\sigma/d\Omega$ , fm <sup>2</sup> /sr	Center-of-mass scattering angle, $\theta_{cm}$ , deg	Differential cross section, $d\sigma/d\Omega$ , fm <sup>2</sup> /sr	Center-of-mass scattering angle, $\theta_{cm}$ , deg	Differential cross section, $d\sigma/d\Omega$ , fm <sup>2</sup> /sr
28.75	0.182 ± 0.002	51.36	0.00667 ± 0.00054	65.64	0.00358 ± 0.00033
36.99	.0672 ± .0014	53.41	.00549 ± .00058	67.67	.00259 ± .00028
41.10	.0244 ± .0008	55.45	.00852 ± .00061	69.70	.00190 ± .00024
43.16	.0149 ± .0008	57.49	.00817 ± .00049	71.72	.000938 ± .000170
45.21	.0171 ± .0010	59.53	.00472 ± .00038	73.75	.00111 ± .00021
47.26	.0193 ± .0009	61.57	.00201 ± .00019	75.77	.00109 ± .00017
49.31	.0151 ± .0010	63.61	.00246 ± .00027		

(e) Inelastic scattering to 2.17-MeV (348-fJ) level

37.00	0.0700 ± 0.0014	51.37	0.0337 ± 0.0012	63.62	0.0106 ± 0.0006
41.12	.0966 ± .0017	53.42	.0316 ± .0014	65.65	.00674 ± .00045
43.17	.0976 ± .0020	55.46	.0189 ± .0009	69.71	.00414 ± .00035
45.22	.0597 ± .0019	59.55	.0115 ± .0006	71.74	.00393 ± .00034
47.28	.0298 ± .0011	61.58	.0138 ± .0006	73.76	.00448 ± .00043
49.33	.0244 ± .0012				

(f) Inelastic scattering to 2.48-MeV (397-fJ) level

37.01	0.0744 ± 0.0014	51.38	0.0268 ± 0.0011	63.63	0.00830 ± 0.00050
41.12	.114 ± .001	53.43	.0218 ± .0012	65.66	.00634 ± .00044
43.18	.0599 ± .0016	55.47	.0146 ± .0008	69.72	.00396 ± .00035
45.23	.0429 ± .0016	59.55	.00952 ± .00053	71.75	.00342 ± .00032
47.28	.0338 ± .0012	61.59	.0111 ± .0006	73.77	.00312 ± .00036
49.33	.0233 ± .0012				

<sup>a</sup>Absolute cross sections obtained by normalizing <sup>113</sup>In elastic to <sup>115</sup>In elastic cross sections.

TABLE V. - DIFFERENTIAL CROSS SECTIONS FOR SCATTERING OF 42-MeV ALPHA PARTICLES BY INDIUM 115

(a) Elastic scattering

Center-of-mass scattering angle, $\theta_{cm}$ , deg	Differential cross section, $d\sigma/d\Omega$ , fm <sup>2</sup> /sr	Center-of-mass scattering angle, $\theta_{cm}$ , deg	Differential cross section, $d\sigma/d\Omega$ , fm <sup>2</sup> /sr	Center-of-mass scattering angle, $\theta_{cm}$ , deg	Differential cross section, $d\sigma/d\Omega$ , fm <sup>2</sup> /sr
31.25	21.9 ± 0.0	47.68	0.600 ± 0.007	61.97	0.124 ± 0.002
33.30	16.2 ± .0	49.73	.695 ± .006	64.01	.0561 ± .0014
35.36	8.57 ± .02	51.77	.563 ± .007	66.04	.0216 ± .0009
37.42	4.24 ± .02	53.82	.301 ± .004	68.07	.0261 ± .0010
39.48	3.55 ± .02	55.86	.126 ± .002	70.09	.0388 ± .0012
41.53	3.25 ± .01	57.90	.122 ± .002	74.14	.0146 ± .0007
43.58	2.00 ± .01	59.94	.153 ± .002	78.18	.0053 ± .0005
45.63	.909 ± .008				

(b) Inelastic scattering to 1.227-MeV (196.6-fJ) 2<sup>+</sup> multiplet

31.26	0.369 ± 0.005	47.70	0.0878 ± 0.0027	62.00	0.0052 ± 0.0005
33.32	.185 ± .003	49.75	.0330 ± .0012	64.03	.0120 ± .0007
35.38	.289 ± .004	51.80	.0170 ± .0012	66.06	.0155 ± .0008
37.44	.286 ± .004	53.84	.0316 ± .0012	68.09	.0111 ± .0006
39.49	.175 ± .004	55.88	.0416 ± .0012	70.12	.0049 ± .0004
41.55	.0689 ± .0021	57.92	.0304 ± .0012	74.17	.0040 ± .0004
43.60	.0746 ± .0024	59.96	.0099 ± .0006	78.21	.0039 ± .0004
45.65	.110 ± .003				

(c) Inelastic scattering to 2.259-MeV (361.9-fJ) 3<sup>-</sup> multiplet

33.33	0.371 ± 0.005	47.72	0.0536 ± 0.0021	62.02	0.0210 ± 0.0010
35.39	.233 ± .004	49.77	.0598 ± .0016	64.05	.0120 ± .0007
37.45	.140 ± .003	51.81	.0529 ± .0021	66.09	.0083 ± .0006
39.51	.154 ± .003	53.86	.0372 ± .0013	68.12	.0060 ± .0005
41.56	.152 ± .003	55.90	.0171 ± .0008	70.15	.0089 ± .0006
43.62	.116 ± .003	57.94	.0222 ± .0009	74.20	.0059 ± .0005
45.67	.0597 ± .0020	59.98	.0214 ± .0009	78.24	.0010 ± .0002

TABLE VI. - DIFFERENTIAL CROSS SECTIONS FOR SCATTERING OF 42-MeV ALPHA PARTICLES BY ANTIMONY 121<sup>a</sup>

(a) Elastic scattering

Center-of-mass scattering angle, $\theta_{cm}$ , deg	Differential cross section, $d\sigma/d\Omega$ , fm <sup>2</sup> /sr	Center-of-mass scattering angle, $\theta_{cm}$ , deg	Differential cross section, $d\sigma/d\Omega$ , fm <sup>2</sup> /sr	Center-of-mass scattering angle, $\theta_{cm}$ , deg	Differential cross section, $d\sigma/d\Omega$ , fm <sup>2</sup> /sr
31.20	32.8 ± 0.1	47.61	0.961 ± 0.008	63.92	0.0602 ± 0.0017
33.25	23.0 ± .0	49.66	1.01 ± .01	65.95	.0296 ± .0012
35.31	12.2 ± .0	51.70	.749 ± .008	67.98	.0433 ± .0013
37.36	6.40 ± .02	53.74	.351 ± .004	70.00	.0504 ± .0014
39.41	5.35 ± .02	55.78	.180 ± .003	72.03	.0362 ± .0012
41.47	4.59 ± .02	57.82	.196 ± .003	74.05	.0138 ± .0008
43.52	2.72 ± .02	59.85	.221 ± .004	76.07	.0057 ± .0004
45.56	1.31 ± .01	61.89	.151 ± .003	78.08	.0108 ± .0008

(b) Inelastic scattering to 0.55-MeV (88.1-fJ) level

31.20	0.0257 ± 0.0017	47.62	0.0069 ± 0.0008	63.93	0.0023 ± 0.0003
33.26	.0305 ± .0018	49.66	.0035 ± .0004	65.96	.0014 ± .0003
35.31	.0429 ± .0021	51.71	.0041 ± .0004	67.99	.00056 ± .00014
37.37	.0370 ± .0019	53.75	.0074 ± .0006	70.01	.00074 ± .00014
39.42	.0099 ± .0010	55.79	.0039 ± .0004	72.04	.00050 ± .00014
41.47	.0099 ± .0010	57.83	.0036 ± .0003	74.06	.00090 ± .00021
43.52	.0117 ± .0010	59.86	.0013 ± .0003	76.08	.00061 ± .00017
45.57	.0200 ± .0014	61.90	.0022 ± .0003	78.10	.00031 ± .00012

(c) Inelastic scattering to 1.1-MeV (176-fJ) level

33.27	0.143 ± 0.009	51.72	0.0158 ± 0.0010	65.97	0.0139 ± 0.0008
37.38	.282 ± .006	53.76	.0305 ± .0012	68.00	.0088 ± .0006
39.43	.163 ± .004	55.80	.0416 ± .0001	70.03	.00211 ± .00031
41.48	.0701 ± .0026	57.84	.0234 ± .0010	72.05	.00182 ± .00028
43.53	.0710 ± .0026	59.87	.0067 ± .0008	74.07	.00385 ± .00041
45.58	.104 ± .003	61.91	.0053 ± .0004	76.09	.00593 ± .00052
47.63	.0749 ± .0022	63.94	.0117 ± .0008	78.11	.00329 ± .00039
49.67	.0309 ± .0012				

<sup>a</sup>Normalized to average elastic tin and tellurium cross sections.

TABLE VI. - Concluded. DIFFERENTIAL CROSS SECTIONS FOR SCATTERING OF  
42-MeV ALPHA PARTICLES BY ANTIMONY 121<sup>a</sup>

(d) Inelastic scattering to 1.4-MeV (224-fJ) level

Center-of-mass scattering angle, $\theta_{cm}$ , deg	Differential cross section, $d\sigma/d\Omega$ , fm <sup>2</sup> /sr	Center-of-mass scattering angle, $\theta_{cm}$ , deg	Differential cross section, $d\sigma/d\Omega$ , fm <sup>2</sup> /sr	Center-of-mass scattering angle, $\theta_{cm}$ , deg	Differential cross section, $d\sigma/d\Omega$ , fm <sup>2</sup> /sr
31.21	0.202 ± 0.004	51.72	0.0180 ± 0.0010	65.98	0.00342 ± 0.00039
33.27	.121 ± .003	53.77	.0098 ± .0007	68.01	.00399 ± .00041
41.49	.0626 ± .0025	55.81	.0089 ± .0008	70.03	.00306 ± .00036
43.54	.0351 ± .0019	57.85	.0089 ± .0007	72.06	.00155 ± .00025
45.59	.0241 ± .0017	59.88	.0057 ± .0006	74.08	.00056 ± .00015
47.63	.0243 ± .0012	61.92	.0044 ± .0004	76.10	.00112 ± .00022
49.68	.0237 ± .0010	63.95	.00227 ± .00031	78.12	.00117 ± .00022

(e) Inelastic scattering to 2.2-MeV (352-fJ) level

51.74	0.0508 ± 0.0018	61.93	0.0222 ± 0.0010	72.08	0.00844 ± 0.00061
53.78	.0342 ± .0012	63.97	.0142 ± .0008	74.10	.00575 ± .00050
55.82	.0228 ± .0012	66.00	.0105 ± .00067	76.12	.00263 ± .00034
57.86	.0232 ± .0010	68.03	.00789 ± .00058	78.14	.00256 ± .00034
59.90	.0252 ± .0013	70.05	.00749 ± .00057		

<sup>a</sup>Normalized to average elastic tin and tellurium cross sections.

TABLE VII. - DIFFERENTIAL CROSS SECTIONS FOR SCATTERING OF 42-MeV ALPHA PARTICLES BY ANTIMONY 123<sup>a</sup>

(a) Elastic scattering

Center-of-mass scattering angle, $\theta_{cm}$ , deg	Differential cross section, $d\sigma/d\Omega$ , fm <sup>2</sup> /sr	Center-of-mass scattering angle, $\theta_{cm}$ , deg	Differential cross section, $d\sigma/d\Omega$ , fm <sup>2</sup> /sr	Center-of-mass scattering angle, $\theta_{cm}$ , deg	Differential cross section, $d\sigma/d\Omega$ , fm <sup>2</sup> /sr
26.59	105 ± 0.2	47.12	0.985 ± 0.017	67.48	0.0423 ± 0.0019
28.65	53.3 ± .1	49.26	1.06 ± .019	69.55	.0434 ± .0023
30.71	36.7 ± .1	51.20	.915 ± .017	71.53	.0458 ± .0028
32.76	27.5 ± .1	53.35	.506 ± .014	73.55	.0208 ± .0018
34.82	16.4 ± .1	55.29	.235 ± .009	75.57	.00906 ± .0012
36.87	8.14 ± .04	57.32	.190 ± .005	77.59	.00673 ± .00107
38.92	5.85 ± .04	59.36	.240 ± .004	79.60	.0127 ± .00147
40.97	5.08 ± .03	61.39	.175 ± .005	81.62	.0113 ± .00138
41.07	4.93 ± .04	63.42	.101 ± .0031	83.63	.00748 ± .00112
43.02	3.39 ± .03	65.45	.0335 ± .0019	85.64	.00323 ± .00073
45.17	1.56 ± .02				

(b) Inelastic scattering to 0.540-MeV (86.5-fJ) level

34.82	0.0487 ± 0.0036	53.26	0.0079 ± 0.0017	69.52	0.00014 ± 0.00014
38.93	.0470 ± .0036	55.30	.0071 ± .0014	71.54	.00017 ± .00017
40.98	.0180 ± .0026	57.33	.0067 ± .0016	73.56	.00050 ± .00031
43.03	.0149 ± .0023	59.37	.00138 ± .00036	75.58	.00186 ± .00056
45.08	.0245 ± .0028	61.40	.00205 ± .00053	77.60	.00050 ± .00031
47.13	.0118 ± .0019	63.44	.00330 ± .00057	79.62	.00033 ± .00023
49.17	.0081 ± .0017	65.47	.00250 ± .00061	85.65	.00050 ± .00031
51.21	.0050 ± .0014	67.49	.00138 ± .00036		

(c) Inelastic scattering to 1.08-MeV (173-fJ) level

34.83	0.196 ± 0.076	55.31	0.0357 ± 0.0034	71.55	0.00119 ± 0.00045
38.94	.204 ± .076	57.34	.0299 ± .0019	73.58	.00223 ± .00056
40.99	.0678 ± .0048	59.38	.0141 ± .0012	75.60	.00321 ± .00069
43.04	.0461 ± .0039	61.41	.0031 ± .0006	77.61	.00447 ± .00087
45.09	.0791 ± .0050	63.45	.0116 ± .00104	79.63	.00135 ± .00048
47.14	.0756 ± .0050	65.47	.0129 ± .00138	81.64	.00071 ± .00034
49.18	.0340 ± .0033	67.50	.0131 ± .0011	83.65	.00050 ± .00031
51.22	.0112 ± .0019	69.53	.00295 ± .00067	85.66	.00104 ± .00042
53.27	.0256 ± .0031				

<sup>a</sup>Normalized to average elastic tin and tellurium cross sections.

TABLE VIII. - SUMMARY OF DATA ON QUADRUPOLE EXCITATIONS IN SILVER

Isotope	Spin and parity, $J^\pi$	Energy, $E^*$		This work		Previous works		
		MeV	fJ	Partial deformation, $\beta_2$	Total deformation, $\beta_2$	Partial deformation, $\beta_2$	Total deformation, $\beta_2$	Reference
Palladium 106	$2^+$	0.513	82.2	----	----	----	0.227	7
<sup>a</sup> Silver 107	$3/2^-$	.318	51.3	0.14	----	0.14	-----	--
<sup>a</sup> Silver 107	$5/2^-$	.423	67.3	.17	----	.17	-----	--
<sup>a</sup> Silver 107	Doublet	.380	60.9	----	0.22	----	.22	--
Cadmium 108	$2^+$	.633	101	----	----	----	.195	7
Palladium 108	$2^+$	.433	69.4	----	----	----	.241	7
<sup>a</sup> Silver 109	$3/2^-$	.300	48.1	.12	----	----	-----	--
<sup>a</sup> Silver 109	$5/2^-$	.409	65.5	.15	----	----	-----	--
<sup>a</sup> Silver 109	Doublet	.380	60.9	----	.19	----	-----	--
Cadmium 110	$2^+$	.656	105	----	----	---	.187	7

<sup>a</sup>All silver energies are accurate to  $\pm 0.015$  MeV ( $\pm 2.4$  fJ).

TABLE IX. - SUMMARY OF DATA ON OCTUPOLE EXCITATIONS  
IN SILVER

Isotope	Spin and parity, $J^\pi$	Energy, $E^*$		This work; partial deformation, $J_f \beta_3$	Previous works		
		MeV	fJ		Partial deformation, $J_f \beta_3$	Total deformation, $\beta_3$	Reference
Palladium 106	$3^-$	2.07	332	-----	----	0.15	9
<sup>a</sup> Silver 107	--	2.17	348	0.10	0.10	----	--
Cadmium 108	$3^-$	----	---	-----	----	----	--
Palladium 108	$3^-$	2.03	325	-----	----	.14	9
<sup>a</sup> Silver 109	--	2.17	348	.084	----	----	--
Cadmium 110	$3^-$	2.05	328	-----	----	.15	10

<sup>a</sup>All silver energies are accurate to  $\pm 0.015$  MeV ( $\pm 2.4$  fJ).

TABLE X. - ENERGY CENTERS OF  
GRAVITY OF COLLECTIVE  
EXCITATIONS IN INDIUM

Isotope	Excitation energy, E* (2 <sup>+</sup> )		Excitation energy, E* (3 <sup>-</sup> )	
	keV	fJ	keV	fJ
Cadmium 112	610	97.7	1968	315.3
<sup>a</sup> Indium 113	1311	210.0	2325	372.5
Tin 114	1300	208.0	2290	366.9
Cadmium 114	555	88.9	1945	311.6
<sup>a</sup> Indium 115	1227	196.6	2259	361.9
Tin 116	1287	206.2	2325	372.5

<sup>a</sup>All indium energies are accurate to  $\pm 0.015$  MeV ( $\pm 2.4$  fJ).

TABLE XI. - ENERGY CENTERS OF  
GRAVITY OF COLLECTIVE  
EXCITATIONS IN ANTIMONY

Isotope	Excitation energy, E* (2 <sup>+</sup> )		Excitation energy, E* (3 <sup>-</sup> )	
	keV	fJ	keV	fJ
Tin 120	1176	188.4	2410	386.1
<sup>a</sup> Antimony 121	1006	161.2	2260	362.1
Tellurium 122	557	89.2	2170	347.7
Tin 122	1123	179.9	2454	393.2
<sup>a</sup> Antimony 123	964	154	-----	-----
Tellurium 124	605	96.9	2300	368

<sup>a</sup>All antimony indium energies are accurate to  $\pm 0.015$  MeV ( $\pm 2.4$  fJ).

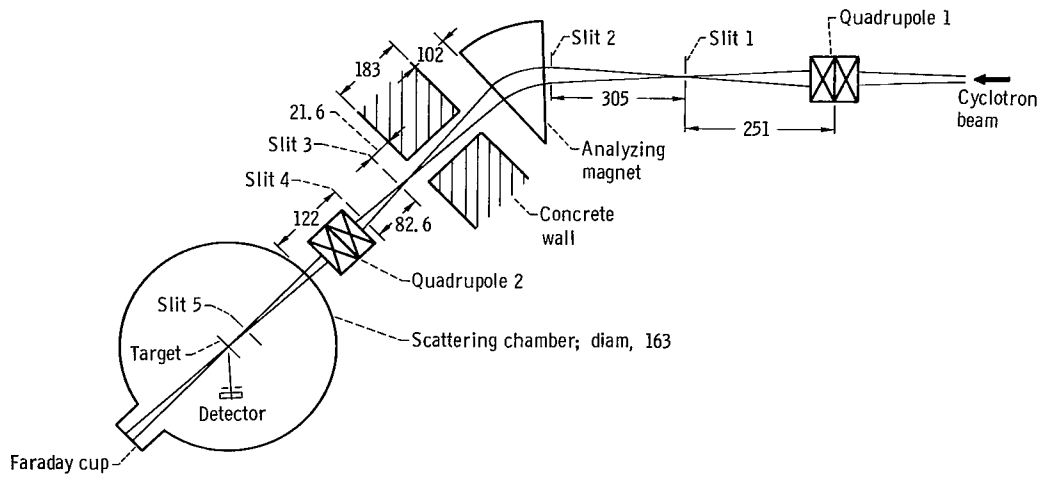


Figure 1. - Schematic diagram of experimental arrangement. (All dimensions are in centimeters.)

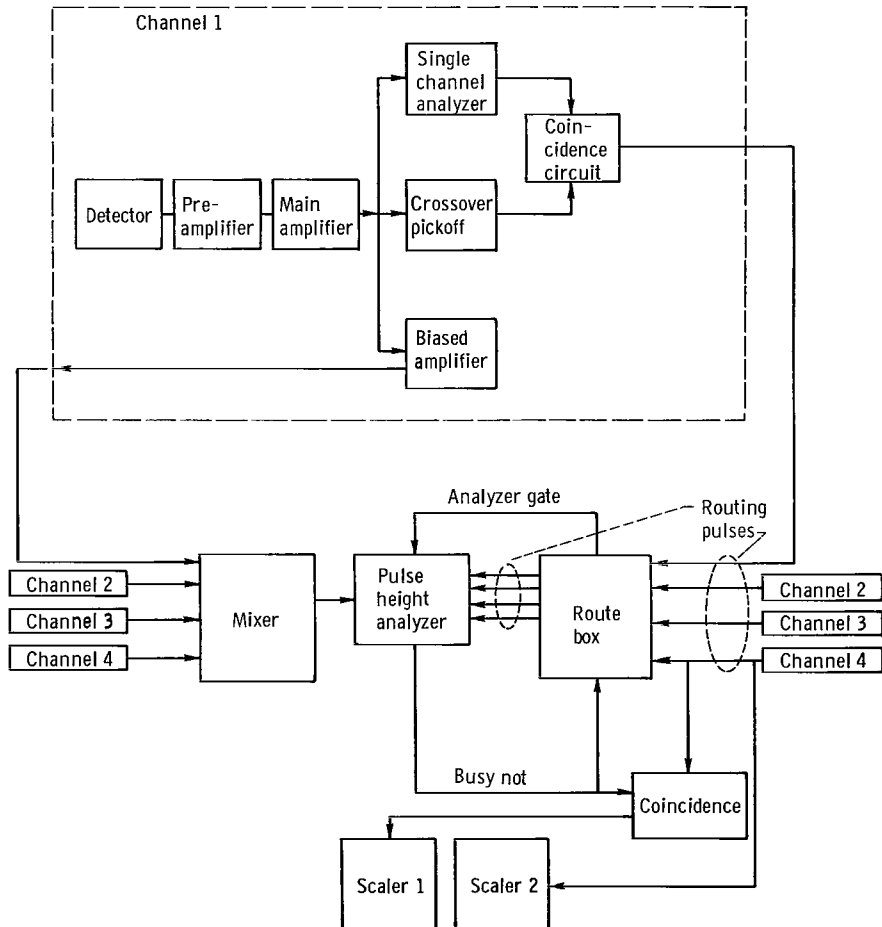
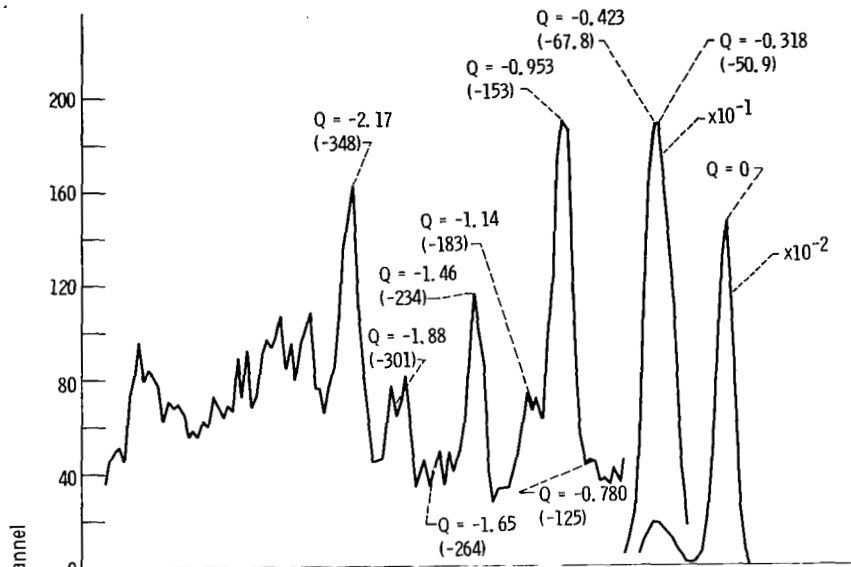
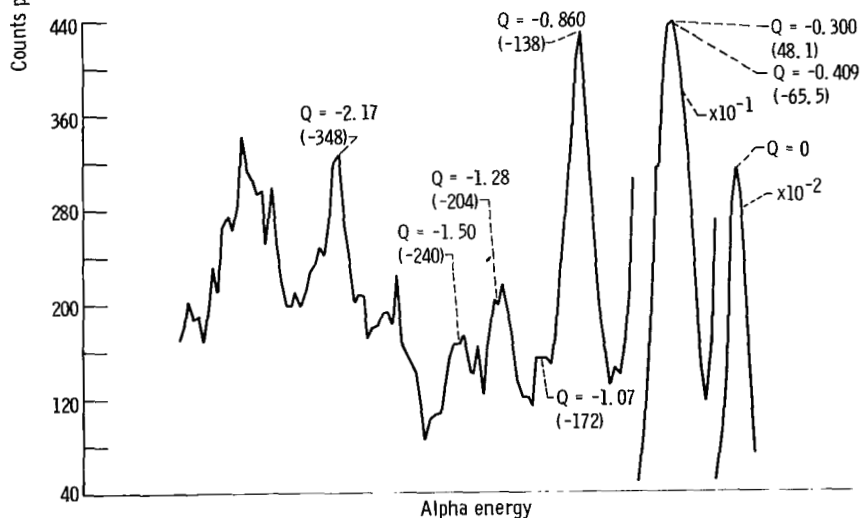


Figure 2. - Block diagram of electronics. (Channel 1 is shown in detail and is representative of channels 2, 3, and 4.)

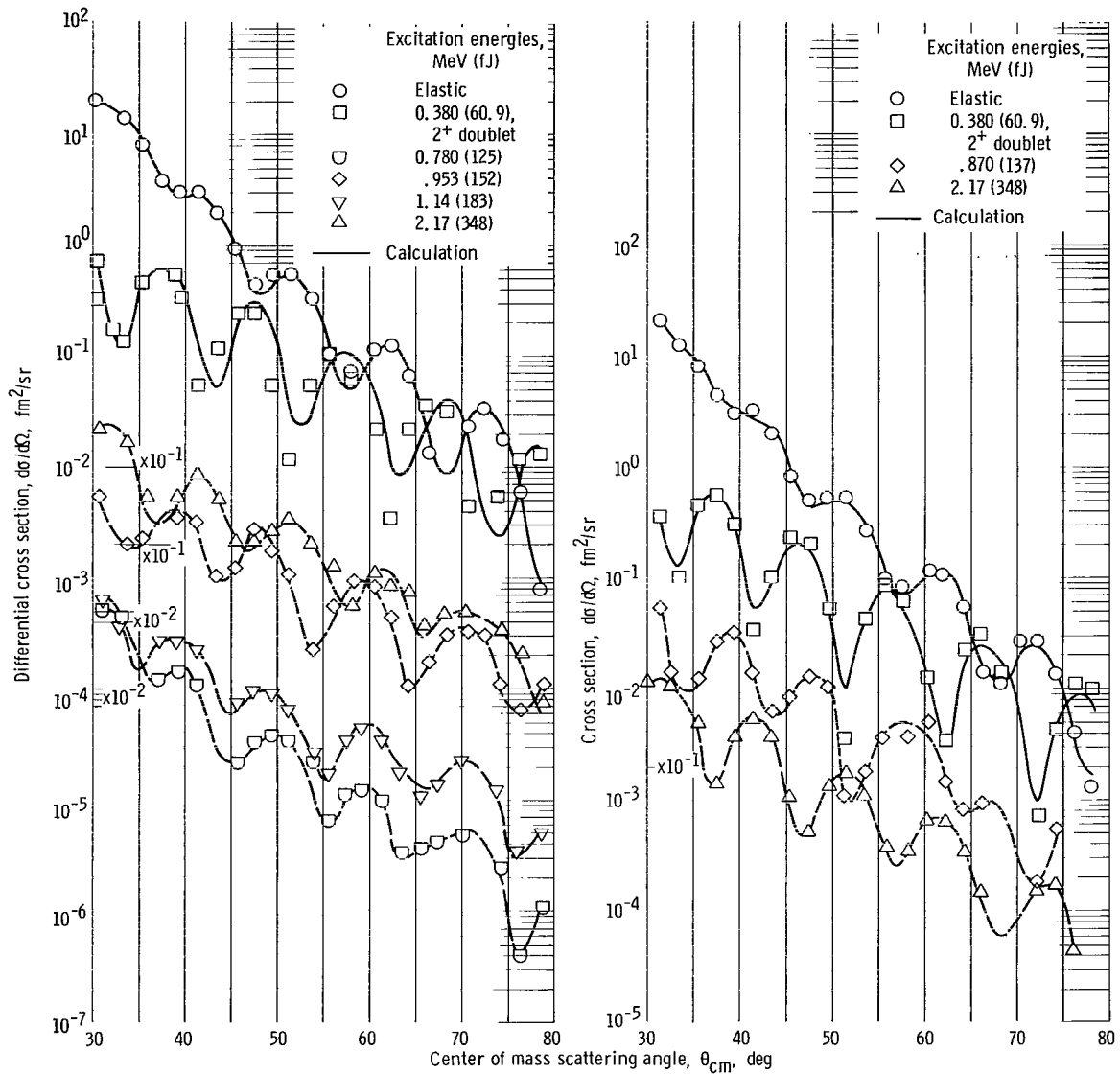


(a) Silver 107 ( $\alpha, \alpha'$ ). Incident charge, 500 microcoulombs.



(b) Silver 109 ( $\alpha, \alpha'$ ). Incident charge, 400 microcoulombs.

Figure 3. - Typical silver energy spectra. Laboratory scattering angle,  $36^\circ$ . (All energies are in MeV (fJ)).



(a) Silver 107.

(b) Silver 109.

Figure 4. - Differential cross sections for scattering 42-MeV (6.7 pJ) alpha particles.

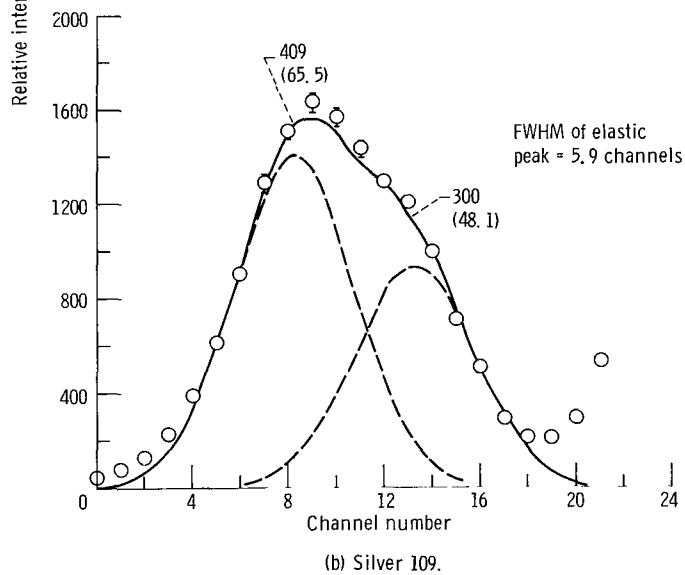
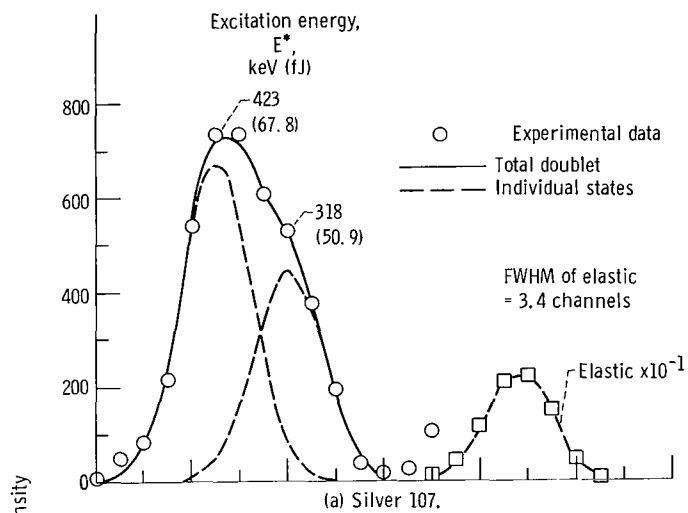
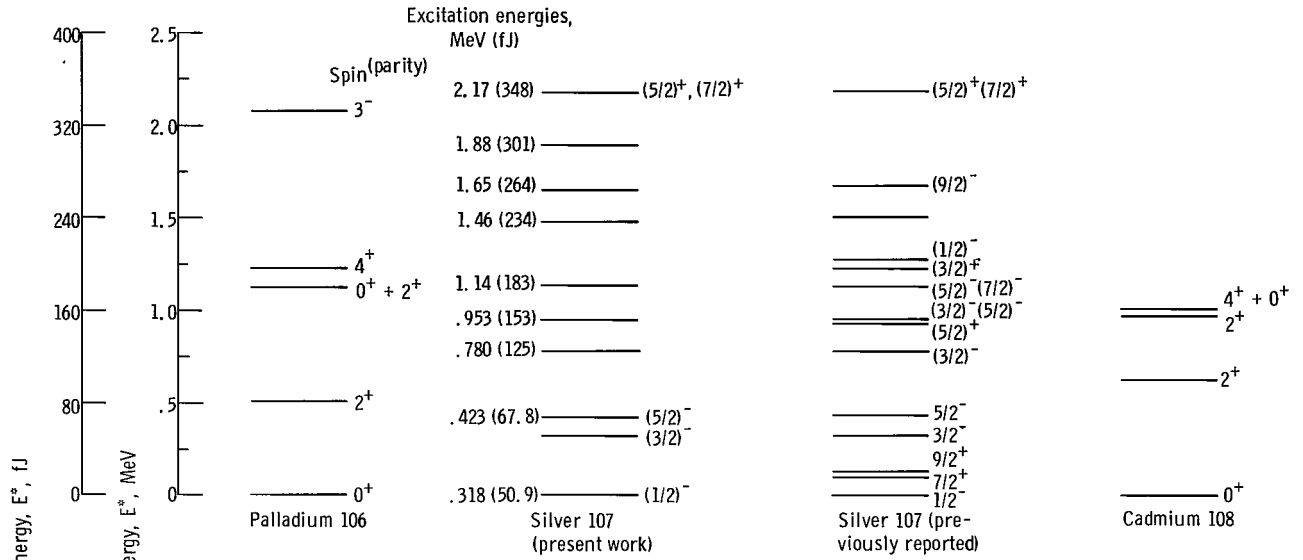
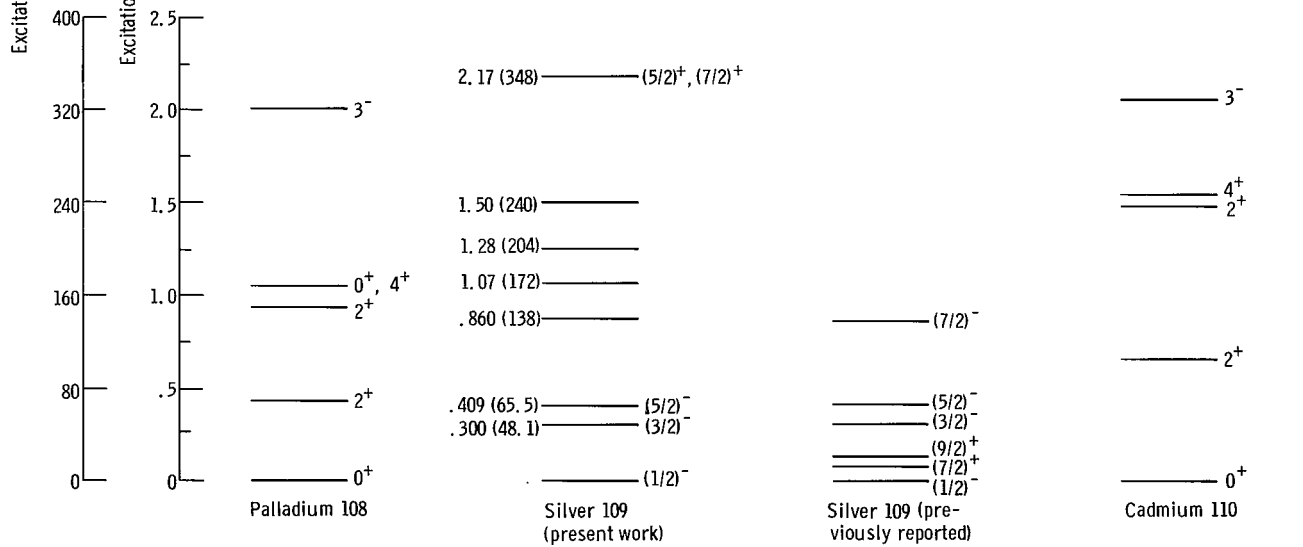


Figure 5. - Analysis of quadrupole doublet.



(a) Silver 107.



(b) Silver 109.

Figure 6. - Energy level diagram summarizing silver data.

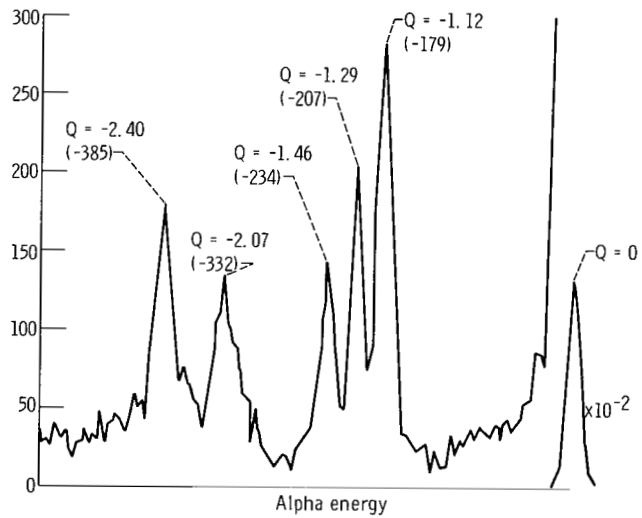
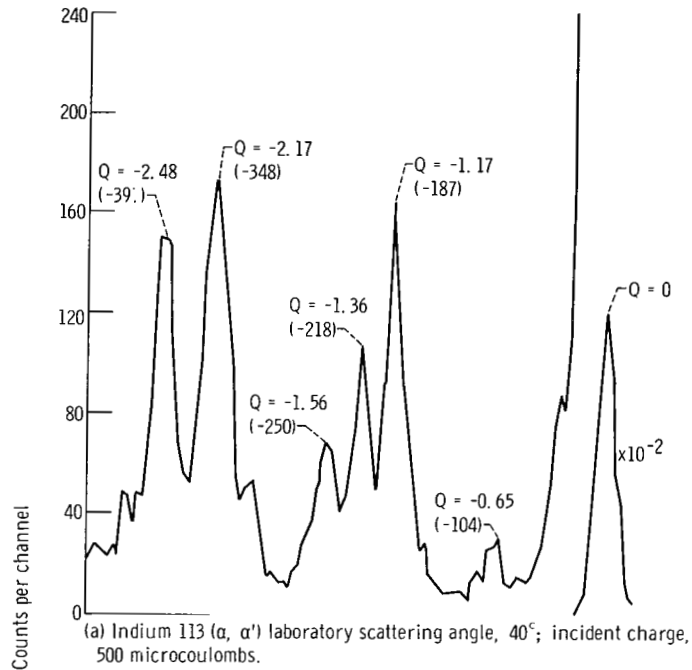


Figure 7. - Typical Indium ( $\alpha$ ,  $\alpha'$ ) energy spectra. (All energies are in MeV (fJ)).

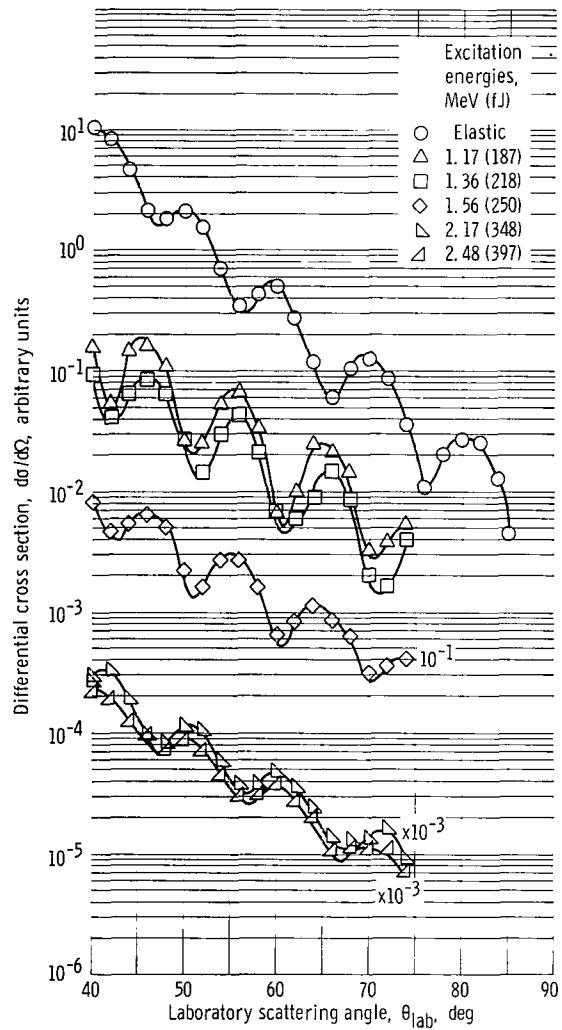


Figure 8. - Cross sections for individual indium 113 peaks.

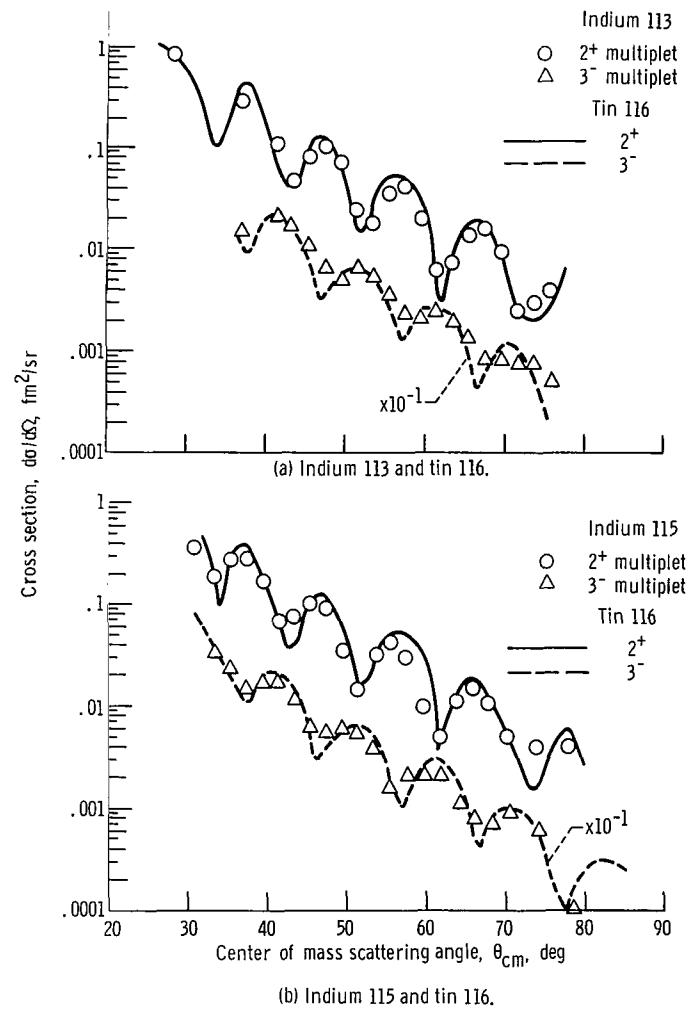


Figure 9. - Comparison of total 2<sup>+</sup> and 3<sup>-</sup> indium multiplet strengths with corresponding tin cross sections.

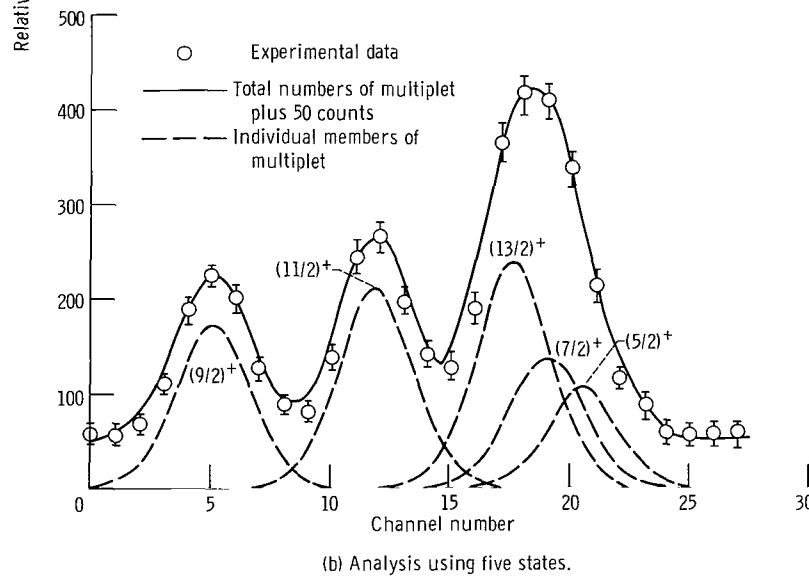
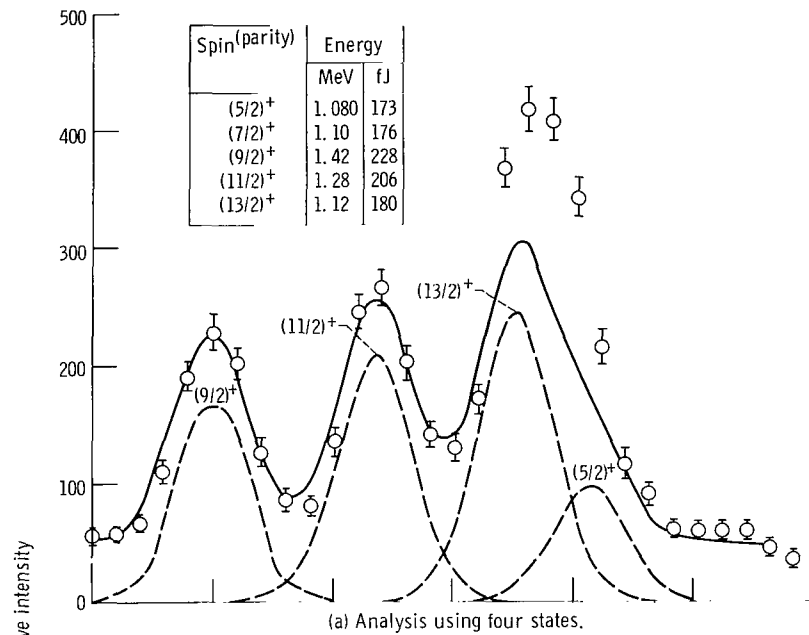


Figure 10. - Analysis of quadrupole multiplet in indium 115.

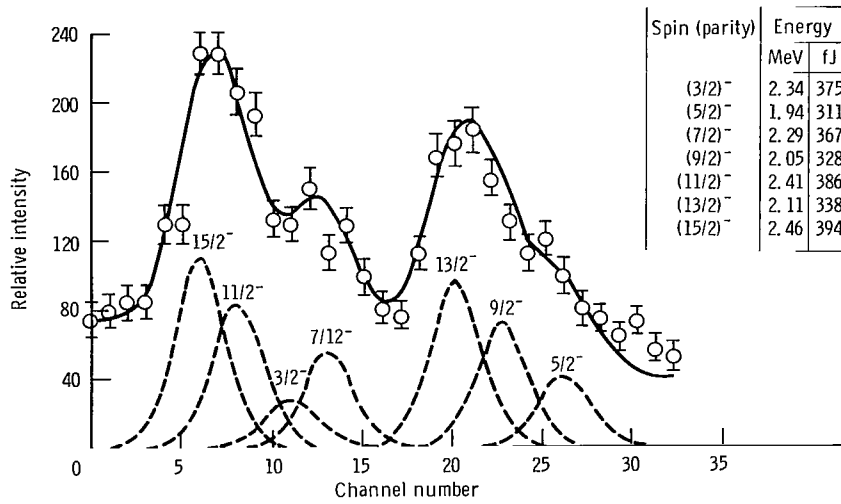


Figure 11. - Analysis of octupole multiplet of indium 115.

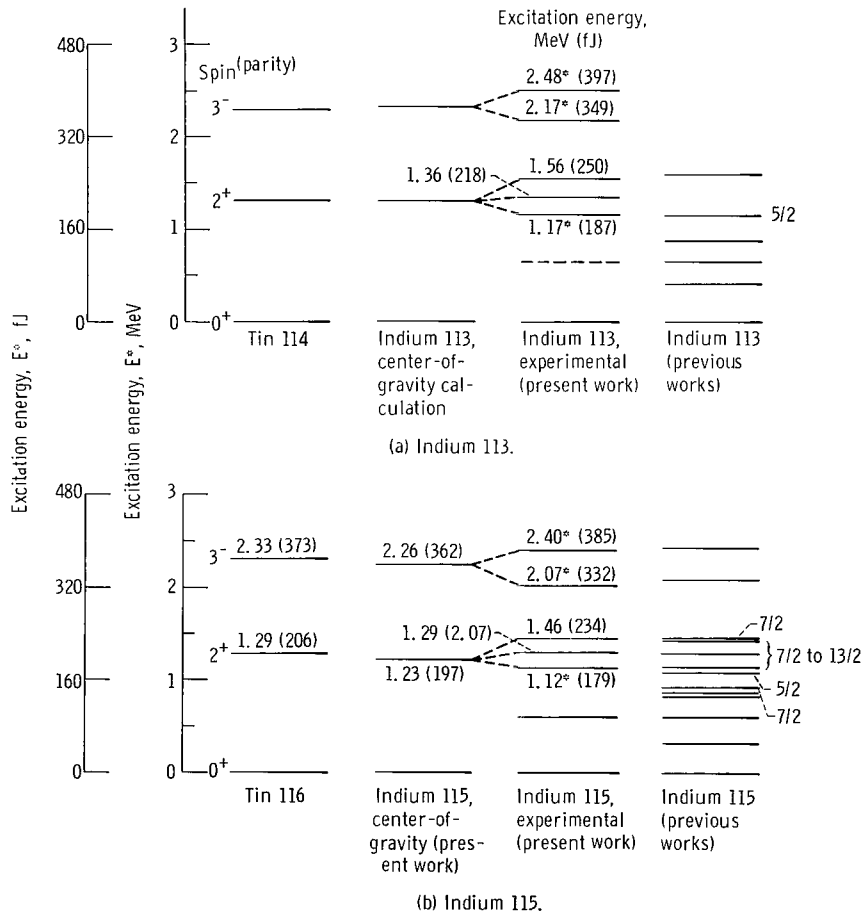


Figure 12. - Level diagram summarizing indium data. (Asterisks indicate unresolved levels.)

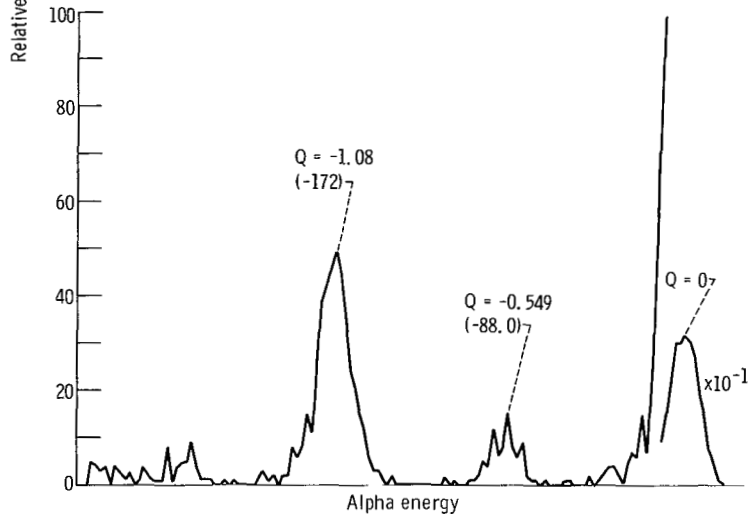
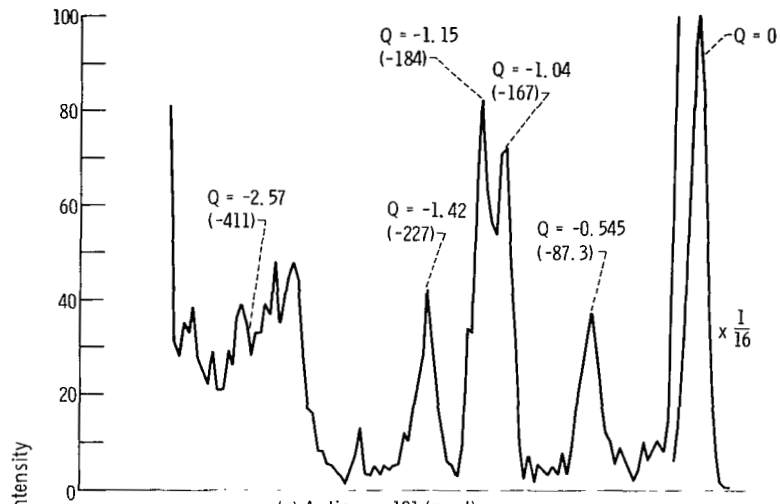
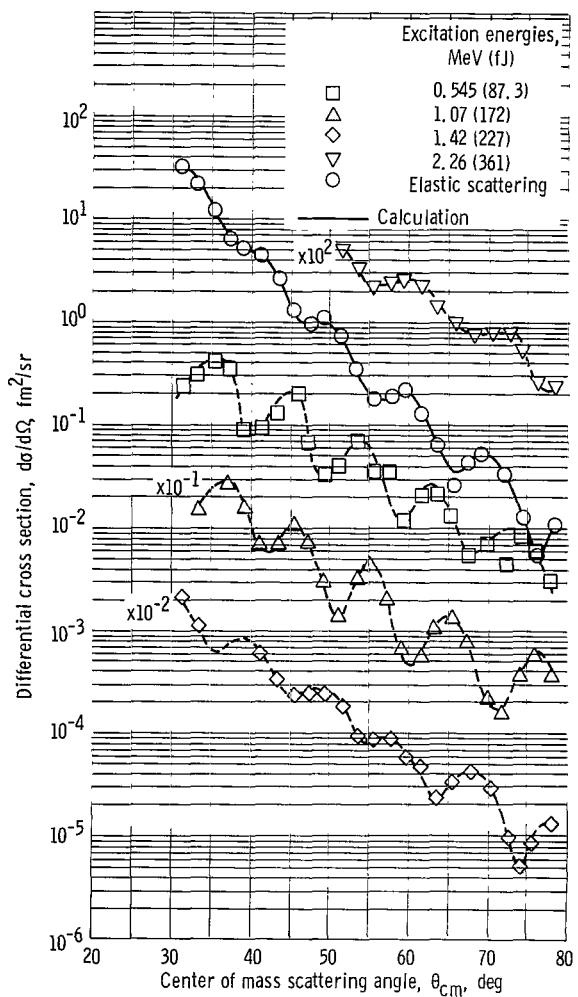
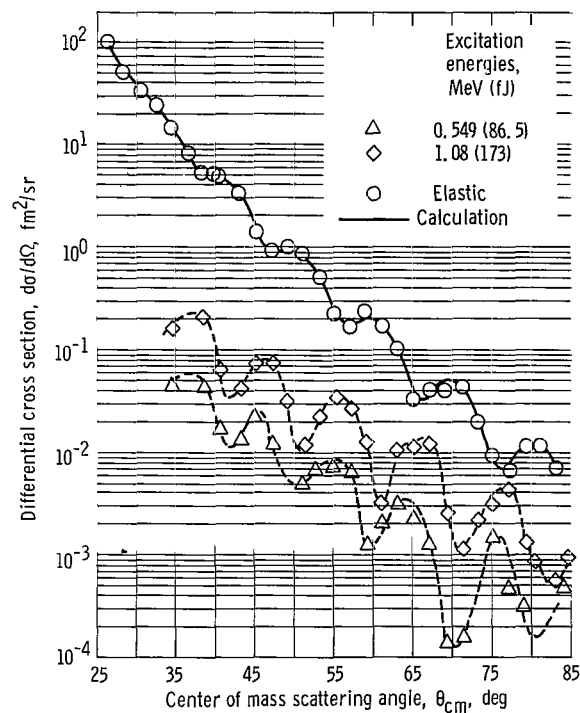


Figure 13. - Typical antimony energy spectra. Laboratory scattering angle,  $52^\circ$ , incident charge, 1000 microcoulombs. (All energies are in MeV (fJ)).



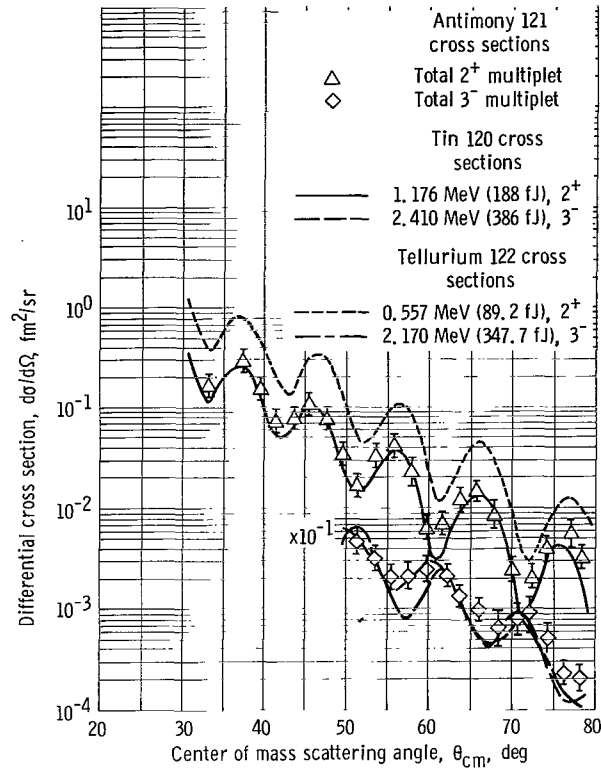
(a) Antimony 121.



(b) Antimony 123.

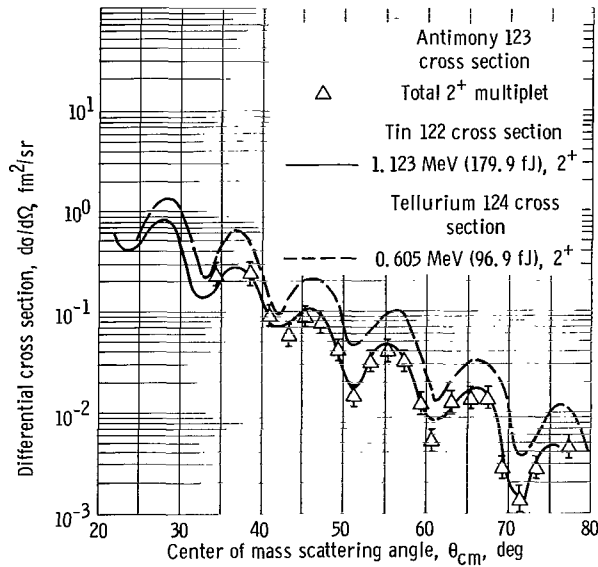
Figure 14. - Concluded.

Figure 14. - Differential cross sections for scattering 42-MeV (6.7 pJ) alpha particles from antimony (normalized to average elastic tin and tellurium cross sections).



(a) Antimony 121, tin 120, and tellurium 122.

Figure 15. - Comparison of total  $2^+$  and  $3^-$  antimony multiplet strengths with corresponding tin and tellurium cross sections.



(b) Antimony 123, tin 122, and tellurium 124.

Figure 15. - Concluded.

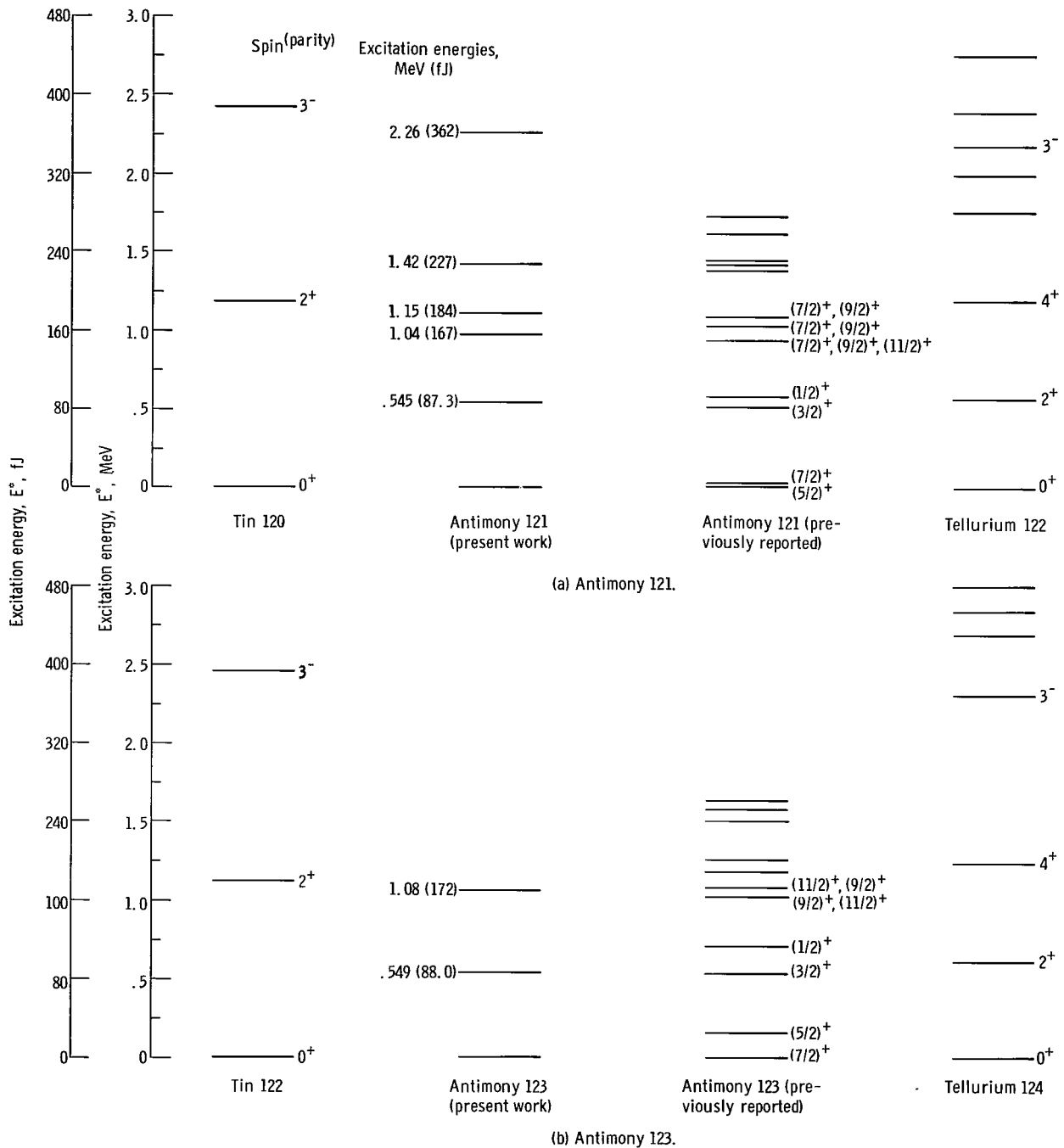


Figure 16. - Energy level diagrams summarizing antimony data.

*"The aeronautical and space activities of the United States shall be conducted so as to contribute . . . to the expansion of human knowledge of phenomena in the atmosphere and space. The Administration shall provide for the widest practicable and appropriate dissemination of information concerning its activities and the results thereof."*

—NATIONAL AERONAUTICS AND SPACE ACT OF 1958

## NASA SCIENTIFIC AND TECHNICAL PUBLICATIONS

**TECHNICAL REPORTS:** Scientific and technical information considered important, complete, and a lasting contribution to existing knowledge.

**TECHNICAL NOTES:** Information less broad in scope but nevertheless of importance as a contribution to existing knowledge.

**TECHNICAL MEMORANDUMS:** Information receiving limited distribution because of preliminary data, security classification, or other reasons.

**CONTRACTOR REPORTS:** Scientific and technical information generated under a NASA contract or grant and considered an important contribution to existing knowledge.

**TECHNICAL TRANSLATIONS:** Information published in a foreign language considered to merit NASA distribution in English.

**SPECIAL PUBLICATIONS:** Information derived from or of value to NASA activities. Publications include conference proceedings, monographs, data compilations, handbooks, sourcebooks, and special bibliographies.

**TECHNOLOGY UTILIZATION PUBLICATIONS:** Information on technology used by NASA that may be of particular interest in commercial and other non-aerospace applications. Publications include Tech Briefs, Technology Utilization Reports and Notes, and Technology Surveys.

*Details on the availability of these publications may be obtained from:*

SCIENTIFIC AND TECHNICAL INFORMATION DIVISION  
NATIONAL AERONAUTICS AND SPACE ADMINISTRATION  
Washington, D.C. 20546

